through only a portion of the total temperature drop across the contact.) Taking reasonable values for σ and κ at liquid-helium temperatures (assuming the normal metal is copper), we find $P=10^{-5}$ watt, $\Delta T=10^{-2}$ degree.

The above circuit will increase the current density through the superconducting whisker from zero to 10^9 amp/cm^2 in 10^{-10} sec. Thus the current rises so fast that the whisker does not go normal at all. Rather the low-current superconducting state "decays" directly into the high-current superconducting state. It should be pointed out that the circuit constants have to be changed if we wish to reverse the above procedure and go from the high-current state to the low-current state by opening the switch. This is because the decay time ξ_0/s for the high-current state is a couple orders of magnitude smaller than that for the low-current state, a fact which follows from the reciprocal dependence of ξ_0 upon the half energy gap ϵ_0. It appears that the circuit of Fig. 3 offers a practical experimental arrangement for achieving high-current superconductivity.

In conclusion, we mention one possible application. Imagine an elongated loop of wire containing a persistent current in the high-current superconducting state at room temperature. The loop will act like a zero-resistance passive element for external currents fed in one end of the loop and out the other, provided the external currents are much smaller than the internal persistent current (thus insuring that the external currents do not upset the high-current superconducting state). In effect we have a room-temperature zero-resistance transmission line.

PHYSICAL REVIEW VOLUME 116, NUMBER 6 DECEMBER 15, 1959

Calculation of the Cohesive Energy of Metallic Iron

FRANK STERN
United States Naval Ordnance Laboratory, White Oak, Silver Spring, Maryland
(Received July 20, 1959)

The cohesive energy of metallic iron is calculated for the body-centered cubic structure in a singlet spin state at 0°K. The potential field acting on each electron is taken to be that of the ion core and of the remaining valence electrons in the same lattice cell; thus the calculation becomes equivalent to one for the free atom as the lattice constant is increased. Tight-binding wave functions are used, but they are modified by expanding the contributions from neighboring atoms in a power series within a cell, and orthogonalizing to core states. Evaluating the complete wave function in each cell eliminates the need for multicenter integrals otherwise required in the tight-binding method. The wave functions for wave vectors in directions of high symmetry have a rather simple form, and can be described by a few parameters. States near the bottom of the $3d$ band tend to have a more diffuse charge distribution than do the states near the top of the band. Thus the x-ray scattering factor per electron for a partially filled $3d$ band will be less than that for a full band. Calculations of the energy of the solid are made for three values of the atomic sphere radius, r_s, using atomic wave functions from the $3d^74s$ configuration. The indicated configuration in the solid is close to $3d^74s$, making the calculation approximately self-consistent. The calculated width of the occupied portion of the $3d$ band is 0.33 ry. We find the cohesive energy of metallic iron to be 0.43 ± 0.2 ry per atom, which is consistent with the experimental value, 0.32 ry. The equilibrium lattice constant and the compressibility are both found to be in good agreement with experiment. An attempt to replace the Coulomb hole used in the main calculation by an exchange hole, using a single Slater determinant wave function, gave far too little binding.

1. INTRODUCTION AND OUTLINE

1.1 Introduction

ENERGY considerations have long played an important role in physical calculations, and the energy of a system is a particularly important quantity in quantum mechanics. Thus the modern development of solid-state physics is based in part on successful calculations of the cohesive energy of alkali metals. In spite of the importance of cohesive energy calculations, they have been carried out for only a relatively small class of solids. The cellular method was applied first to sodium,[1] and has since been extended with many refinements to other alkali metals. The quantum defect method eliminates the need for constructing a potential function; it has been applied to the alkali metals with good success,[2] and also to the noble metals.[3] A detailed calculation of the energy of beryllium was made by Herring and Hill,[4] and cruder calculations for other metals were carried out by Raimes.[5] Statistical methods have also been applied to a number of elements.[6]

The methods used for calculating the cohesive energy of nonmetals are somewhat different from those applied to metals. The method of linear combination of atomic orbitals has been applied to ionic crystals with con-

[1] E. Wigner and F. Seitz, Phys. Rev. **43**, 804 (1933); **46**, 509 (1934).

[2] H. Brooks and F. S. Ham, Phys. Rev. **112**, 344 (1958).
[3] K. Kambe, Phys. Rev. **99**, 419 (1955).
[4] C. Herring and A. G. Hill, Phys. Rev. **58**, 132 (1940).
[5] S. Raimes, Phil. Mag. **41**, 568 (1950); **43**, 327 (1952); Proc. Phys. Soc. (London) **A66**, 949 (1953).
[6] P. Gombás, *Die Statistische Theorie des Atoms und ihre Anwendungen* (Springer-Verlag, Vienna, 1949). See also a number of later papers in Acta Phys. Hung.

siderable success.[7,8] A technique involving two-electron orbitals was developed by Schmid for diamond,[9] and has been used for zincblende.[10]

In contrast to the fairly limited work on cohesive energy, many methods, some of them quite powerful, have been developed for calculating one-electron energies in solids. There are a number of reviews of band structure methods and results,[11] and new methods are being evolved.[12] Callaway[13] summarizes both the band structure work and the cohesive energy calculations. Slater[14] gives a comprehensive review of the electronic structure of solids.

1.2 Outline of the Calculation

In the present work we propose to show the feasibility of cohesive energy calculations for transition metals, and in particular for iron. We calculate the cohesive energy of body-centered cubic iron at absolute zero, for a singlet spin state. We have not attempted to account for the ferromagnetism of iron, nor do we try to predict the crystal structure of lowest energy. The energy difference between the ferromagnetic and the nonmagnetic state, or between two crystal structures, is much smaller than the cohesive energy. A calculation which attempts to account for these differences might well be an order of magnitude more difficult than the present one. For this reason we restrict our attention to the nonmagnetic state, and to the observed structure. Most of the methods used here have been described previously.[15]

An important feature of this calculation is the assumption that each cell of the crystal is neutral, i.e., that the potential acting on one of the valence electrons is that of the ion core and of the remaining valence electrons in the same cell. This is not exact, since the electron will exclude charge from a region centered at its own position rather than at the center of the cell. We neglect the potential in one cell of the lattice resulting from the charges in neighboring cells and, for most purposes, assume the lattice cell and the potential energy to have spherical symmetry.

Two major simplifications result from the approximation that each cell of the crystal is neutral. First, we can treat each cell of the solid as a unit. This makes the calculation of the energy of the solid quite similar to the corresponding calculation for the free iron atom, and can lead to a cancellation of errors when the difference of these two quantities is taken to find the cohesive energy. The second advantage is that our approximation remains valid for large lattice constants. This is important, since the $3d$ shells on neighboring atoms in metallic iron overlap very little and are—in effect—far apart. Treatments involving an exchange hole can lead to difficulties at large lattice constants[16]; these difficulties are avoided here.

An innovation in our work is a new treatment of the tight-binding method. The small overlap of neighboring $3d$ wave functions makes this method suitable for transition metals. In order to avoid the multicenter integrals usually required,[7,17] we use the tight-binding Bloch wave function in a somewhat modified form. In the atomic cell centered at the origin, the tight-binding wave function is equal to the local atomic orbital plus contributions from all neighboring atoms[17]:

$$\Phi_a(\mathbf{k},\mathbf{r})=\psi_a(\mathbf{r})+\sum_{r_n\neq 0}\exp(i\mathbf{k}\cdot\mathbf{r}_n)\psi_a(\mathbf{r}-\mathbf{r}_n). \quad (1)$$

We depart from the conventional treatment by expanding the contribution of the neighboring atoms in a power series in $\mathbf{r}$. We have done this for both the $3d$ and $4s$ bands in iron, keeping terms through second order in the $3d$ band, and through fourth order in the $4s$ band. We show in Sec. 2.4 how the coefficients in these expansions give information about the energy and charge distribution of the wave function.

Equation (1) applies to the cell at the origin, but in the cell centered at $\mathbf{r}_m$ the wave function differs only by the phase factor $\exp(i\mathbf{k}\cdot\mathbf{r}_m)$ from its value at the corresponding point in the central cell. The tight-binding wave function as actually used has been orthogonalized to the core wave functions.

The approximation we use replaces the exchange and correlation holes by the Coulomb hole resulting from the condition that each lattice cell be neutral. Thus we need find only the kinetic and potential energy in calculating the band structure. These energy integrals can be evaluated in a single lattice cell using our modified tight-binding wave function, and do not require multicenter integrals. Note that, as in the standard tight-binding treatment, we do not solve the Schrödinger equation, but simply find the energy of a predetermined Bloch wave function based on atomic orbitals.

We must exercise some caution in evaluating the kinetic energy in a single cell, since the Laplacian operator is no longer Hermitian when a finite boundary is present unless we restrict ourselves to exact Bloch

[7] P.-O. Löwdin, *Advances in Physics*, edited by N. F. Mott (Taylor and Francis, Ltd., London, 1956), Vol. 5, p. 1.
[8] L. P. Howland, Phys. Rev. **109**, 1927 (1958).
[9] L. A. Schmid, Phys. Rev. **92**, 1373 (1953).
[10] S. Asano and Y. Tomishima, J. Phys. Soc. (Japan) **11**, 644 (1956).
[11] J. R. Reitz, in *Solid-State Physics*, edited by F. Seitz and D. Turnbull (Academic Press, Inc., New York, 1955), Vol. 1, p. 1; F. Herman, Revs. Modern Phys. **30**, 102 (1958).
[12] J. C. Phillips, Phys. Rev. **112**, 685 (1958).
[13] J. Callaway, in *Solid-State Physics*, edited by F. Seitz and D. Turnbull (Academic Press, Inc., New York, 1958), Vol. 7, p. 99.
[14] J. C. Slater, in *Encyclopedia of Physics*, edited by S. Flügge (Springer-Verlag, Berlin, 1956), Vol. 19, p. 1.
[15] F. Stern, Ph.D. thesis, Princeton, 1955 (unpublished).
[16] F. Seitz, *The Modern Theory of Solids* (McGraw-Hill Book Company, Inc., New York, 1940), pp. 334–339. See also p. 111 of reference 14.
[17] The tight-binding method originated with F. Bloch, Z. Physik **52**, 555 (1928). See also N. F. Mott and H. Jones, *The Theories of the Properties of Metals and Alloys* (Oxford University Press, London, 1936), pp. 65–76.

wave functions. For a less restrictive class of wave functions we must use the kinetic energy operator:

$$T=-(\hbar^2/2m)\Delta+(\hbar^2/2m)\delta(\mathbf{n})(\partial/\partial n), \quad (2)$$

where Δ is the Laplacian operator, and the delta function indicates that the normal derivative $\partial/\partial n$ is evaluated on the surface of the cell. The second term, the boundary correction, plays a rather important role in energy calculations in solids. It has been used, directly or indirectly, by many authors, and will be discussed more fully in Sec. 4.1.

The total energy of the solid is not simply the sum of one-electron energies, since this would count interactions between pairs of valence electrons too often. Upon subtracting the extra interactions both in the solid and in the free atom, we find the cohesive energy of the solid to be the small difference of two large numbers. This makes calculations of cohesive energy for many-electron atoms quite difficult.

We have summarized the main steps and some of the principles of our calculation in the foregoing. The details will be presented in the following sections. First we describe the modified tight-binding wave function. In Sec. 3 the potential field is constructed. The following section presents the boundary correction to the Hamiltonian, and finds the one-electron energies in metallic iron. The cohesive energy of the solid is found in Sec. 5, which completes the main calculation. An alternative method of calculation, which replaces the neutrality condition in each cell by the exchange and correlation holes, is given in Sec. 6.

Unless otherwise specified, the unit of distance is the Bohr radius, 0.529×10^{-8} cm, and the unit of energy is the Rydberg, i.e., the ionization energy of hydrogen with a nucleus of infinite mass. One ry equals 13.60 ev. In these units all electrostatic energies contain a factor 2; for example the repulsive energy between two electrons separated by a distance R is $2/R$. All wave functions and charge densities in our work are normalized to 4π in the atomic cell unless otherwise stated.

2. THE MODIFIED TIGHT-BINDING WAVE FUNCTION

2.1 Description of the Method[18]

For solids in which the overlap between wave functions on neighboring atoms is small, the tight-binding,[17] or LCAO (linear combination of atomic orbitals) method[7] is well suited for finding the properties of the crystal if the atomic wave functions are known. The unnormalized Bloch wave function constructed from the atomic orbital $\psi_a(\mathbf{r})$ is

$$\Phi_a(\mathbf{k},\mathbf{r})=\sum \exp(i\mathbf{k}\cdot\mathbf{r}_n)\psi_a(\mathbf{r}-\mathbf{r}_n), \quad (3)$$

where $\mathbf{k}$ is the wave vector and the $\mathbf{r}_n$ are lattice points. For each atomic state a there is a band in the solid with as many discrete values of $\mathbf{k}$ as there are lattice points. In general, these bands will overlap, and matrix elements of the Hamiltonian between tight-binding wave functions belonging to different bands must be evaluated.

One-electron energies in the tight-binding method are integrals of the form $\int\Phi^*H\Phi d\tau/\int\Phi^*\Phi d\tau$, where H is the one-electron Hamiltonian. The integrals are to be evaluated throughout the crystal but have the same value in each lattice cell because the integrands have the periodicity of the lattice. In the conventional tight-binding method[17,7] the expansion of Eq. (3) is substituted for Φ, and gives rise to multicenter integrals. We modify the tight-binding method by evaluating Φ directly in each lattice cell, and we use a Coulomb hole in the cell in place of the exchange and correlation holes. Under these conditions all contributions to the one-electron energy can be calculated in a single lattice cell.

If we place the origin at the center of the cell in which we work, then the tight-binding wave function can be written:

$$\Phi_a(\mathbf{k},\mathbf{r})=\psi_a(\mathbf{r})+\Phi_a'(\mathbf{k},\mathbf{r}), \quad (4)$$

$$\Phi_a'(\mathbf{k},\mathbf{r})=\sum' \exp(i\mathbf{k}\cdot\mathbf{r}_n)\psi_a(\mathbf{r}-\mathbf{r}_n), \quad (5)$$

where the primed summation over $\mathbf{r}_n$ in Eq. (5) excludes the origin. Thus the computation of the tight-binding wave function requires only the evaluation of the overlap contribution from atoms outside the central cell.

The wave function of Eq. (4) must be orthogonalized to the core states in the atomic sphere before it can be used to find one-electron energies. This is necessary if determinant wave functions are used,[19] and is also required in our case to prevent mixing core wave functions and energies with those of the valence bands. We need only orthogonalize Φ_a' to the core wave functions, since we use self-consistent atomic orbitals which have already been orthogonalized to each other.[20] The wave function we use in energy calculations is:

$$\Psi_a(\mathbf{k},\mathbf{r})=\psi_a(\mathbf{r})+\Psi_a'(\mathbf{k},\mathbf{r}), \quad (6)$$

where the overlap term Ψ_a' is orthogonalized to the normalized core states ψ_b:

$$\Psi_a'(\mathbf{k},\mathbf{r})=\Phi_a'(\mathbf{k},\mathbf{r})-\sum_b \psi_b(\mathbf{r})\int\Phi_a'(\mathbf{k},\mathbf{r})\psi_b(\mathbf{r})d\tau. \quad (7)$$

We evaluate $\Phi_a'(\mathbf{k},\mathbf{r})$ first, and orthogonalize it using Eq. (7).

A complete expansion of $\Phi_a'(\mathbf{k},\mathbf{r})$ contains an infinite series of functions of $\mathbf{k}$ and r, each multiplied by a spherical harmonic of appropriate symmetry, and obeys the proper symmetry relations at the surface of the atomic polyhedron.[21] Our simplified expansion of the

[18] A brief account of this method has been presented previously; see F. Stern, Bull. Am. Phys. Soc. 4, 276 (1959).

[19] D. R. Hartree, *The Calculation of Atomic Structures* (John Wiley and Sons, Inc., New York, 1957), p. 42.

[20] F. Stern, Phys. Rev. **104**, 684 (1956).

[21] J. C. Slater, Phys. Rev. **45**, 794 (1934).

TABLE I. Harmonic polynomials of order 0, 1, and 2 belonging to representations of the group of the wave vector $\mathbf{k}$ for symmetry points of the Brillouin zone in face-centered cubic reciprocal lattices. Functions in brackets are degenerate. The lattice constant of the body-centered space lattice is a, and other notation is from Bouckaert *et al.*[a]

Symmetry point	Representation	Harmonic polynomial
Γ: (0,0,0)	Γ_1	1
	Γ_{12}	$[2z^2-x^2-y^2,\ x^2-y^2]$
	$\Gamma_{25'}$	$[xy,\ yz,\ zx]$
$(0,0,k)$	Δ_1	$1,\ z,\ 2z^2-x^2-y^2$
Δ: $k<2\pi/a$	Δ_2	x^2-y^2
	$\Delta_{2'}$	xy
	Δ_5	$[x+y,\ x-y]\ [xz+yz,\ xz-yz]$
H: $k=2\pi/a$	$H_1,\ H_{12},\ H_{25'}$	Same as $\Gamma_1,\ \Gamma_{12},\ \Gamma_{25'}$
$(k/\sqrt{3},\ k/\sqrt{3},\ k/\sqrt{3})$	Λ_1	$1,\ x+y+z,\ xy+yz+zx$
Λ: $k<\pi\sqrt{3}/a$	Λ_3	$[x-y,\ x+y-2z],\ [xz-yz,\ xz+yz-2xy]$
		$[2z^2-x^2-y^2,\ x^2-y^2]$
P: $k=\pi\sqrt{3}/a$	P_1	1
	P_3	$[2z^2-x^2-y^2,\ x^2-y^2]$
	P_4	$[x,\ y,\ z]\ [xy,\ yz,\ zx]$
$(k/\sqrt{2},\ k/\sqrt{2},\ 0)$	Σ_1	$1,\ x+y,\ xy,\ 2z^2-x^2-y^2$
Σ: $k<\pi\sqrt{2}/a$	Σ_2	$xz-yz$
	Σ_3	$z,\ xz+yz$
	Σ_4	$x-y,\ x^2-y^2$
N: $k=\pi\sqrt{2}/a$	$N_{1,2,3,4}$	Same as $\Sigma_{1,2,3,4}$, but without linear terms

[a] See reference 22.

overlap contribution to the wave function is a power series, in which terms are calculated only through second order in most cases. Thus some accuracy is sacrificed to gain considerable simplicity.

The formal expression for the power series expansion of the overlap contribution to the wave function is, to second order:

$$\Phi_a'(0)+\sum_i x_i(\partial\Phi_a'/\partial x_i)_{r=0} +\tfrac{1}{2}\sum_{i,j} x_ix_j(\partial^2\Phi_a'/\partial x_i\partial x_j)_{r=0}, \quad (8)$$

where x_1, x_2, x_3 are used in place of x, y, z, and the derivatives are to be evaluated at the origin of the central cell. The extension to higher powers is obvious. A simple example of one term in Eq. (8) is the coefficient of z in the expansion of Φ_0':

$$(\partial\Phi_0'/\partial z)_{r=0}=\sum_{n\neq 0}(-z_n/r_n)R_{4s}'(r_n)\exp(i\mathbf{k}\cdot\mathbf{r}_n), \quad (9)$$

where $R_{4s}'(r)$ is the derivative of the atomic $4s$ radial wave function. The $4s$ band is identified by setting the subscript a in Φ_a' equal to zero; higher values of a denote the $3d$ bands. The second-order coefficients, and the coefficients in the expansion of the $3d$ overlap contributions, are more complicated than (9), but equally straightforward.[15]

2.2 The 3*d* Wave Functions

The particular linear combinations of the five $3d$ atomic orbitals used to calculate the tight-binding wave functions in the $3d$ band are found by considering the symmetry operations which leave the wave vector invariant.[22] In the three directions of high symmetry, $\langle 001\rangle$, $\langle 111\rangle$, and $\langle 110\rangle$, it is possible to choose the $3d$ orbitals ψ_a so as to eliminate most of the off-diagonal matrix elements of the Hamiltonian.

In Table I we give the harmonic polynomials which belong to particular representations of the group of the wave vector in the three symmetry directions. We follow the notation of reference 22. The results in Table I provide a valuable check on the expansion given in Eq. (8). For example, we see that the wave function contains no first-order terms when the wave vector $\mathbf{k}$ corresponds to the center of the zone, Γ, or to the endpoints of the $\langle 001\rangle$ or $\langle 110\rangle$ axes, H or N. Linear terms may, however, be present at the endpoint of the $\langle 111\rangle$ directions for the representation P_4. Thus the symmetry properties of the wave functions not only allow us to pick the right linear combinations of spherical harmonics from the start, but also allow consistency checks of the numerical work.

The summations over lattice points in Eq. (8) were carried out only for nearest and next-nearest neighbors in finding the wave functions of the $3d$ band. The calculation is rather tedious; some of the details are given elsewhere.[15] The general expression for the unorthogonalized modified tight-binding $3d$ wave function in the solid has the form:

$$\Phi_a(\mathbf{k},\mathbf{r})=R_{3d}(r)Y_{2a}+\sum_{l,j} d_{a,lj}(\mathbf{k})r^lY_{lj}, \quad (10)$$

where $a\geq 1$, and the Y_{lj} are the spherical harmonics of appropriate symmetry defined in Table II. The total number of nonzero coefficients $d_{a,lj}$ is rather small,

[22] Bouckaert, Smoluchowski, and Wigner, Phys. Rev. **50**, 58 (1936).

since we restrict the angular momentum l to values ≤ 2. The wave functions with the largest number of coefficients are Φ_1 and Φ_2 with $\mathbf{k}$ in the $\langle 110\rangle$ directions. In this case $d_{a,00}$, $d_{a,02}$, $d_{a,11}$, $d_{a,21}$, and $d_{a,22}$ may all be nonzero, except that $d_{a,11}=0$ at the points N, where the $\langle 110\rangle$ axes intersect the surface of the Brillouin zone. There are off-diagonal matrix elements connecting Φ_1 and Φ_2, both of which belong to the representation Σ_1 (and N_1). The only other representation in Table I to which two nondegenerate $3d$ wave functions belong is Λ_3. There are matrix elements linking the $3d$ and $4s$ bands in all three symmetry directions, except at the points Γ, H, and P.

To complete the computation of the wave function, we must orthogonalize it to the core, and normalize it. The orthogonalization is accomplished very easily, since the core contains only wave functions of s and p symmetry. We define

$$v_l=r^l-\sum_{n=1}^{3} R_{ns}(r)\int R_{ns}(r)r^{2+l}dr, \quad l=0,2,4\cdots,$$
$$v_l=r^l-\sum_{n=2}^{3} R_{np}(r)\int R_{np}(r)r^{2+l}dr, \quad l=1,3,5\cdots, \tag{11}$$

where the $R_{nl}(r)$ are the core radial wave functions normalized to 4π. In terms of the v_l, our orthogonalized modified tight-binding wave functions for $3d$ electrons are:

$$\Psi_a(\mathbf{k},\mathbf{r})=R_{3d}(r)Y_{2a}+\sum_{l,j} d_{a,lj}(\mathbf{k})v_lY_{lj} +\sum_j d_{a,2j}(\mathbf{k})r^2Y_{2j}, \tag{12}$$

where the first sum includes only $l=0$, 1 and the coefficients are the same as those in Eq. (10). To illustrate these expressions we give the expansions for $\Psi_3(N,\mathbf{r})$ and $\Psi_1(N,\mathbf{r})$, the wave functions of highest and of lowest energy, respectively, in the $3d$ band at N, the endpoint of the [110] direction in the Brillouin zone.[23] They are given for $r_s=2.66$, and are normalized to 4π in the atomic sphere.

$$\Psi_3(N,\mathbf{r})=1.187[R_{3d}(r)-0.02433r^2]Y_{23}, \tag{13}$$
$$\Psi_1(N,\mathbf{r})=0.857\{[R_{3d}(r)+0.01273r^2]Y_{21} -0.2182v_0-0.00096v_2-0.01862r^2Y_{22}\}. \tag{14}$$

The s-like portion of Ψ_1 contributes 18% of the charge density of this wave function. A number of qualitative conclusions can be drawn from the coefficients in Eqs. (13) and (14). This is done in Sec. 2.4.

[23] Use of a particular direction, like [110], instead of all equivalent $\langle 110\rangle$ directions, does not imply lack of full cubic symmetry. It is required by the particular choices made in Tables I and II. Translation to other choices is easily made. For example, when $\mathbf{k}$ is in the [011] direction, the $3d$ function belonging to the representation Σ_2 has an angular dependence given by $yx-zx$ instead of $xz-yz$.

TABLE II. List of the spherical harmonics Y_{lj} of order 0, 1, and 2 used in this work. They are normalized to 4π on the unit sphere.

$Y_{00}=1$	$r^2Y_{21}=(15)^{\frac{1}{2}}xy$
	$r^2Y_{22}=(5/4)^{\frac{1}{2}}(2z^2-x^2-y^2)$
$rY_{11}=(3/2)^{\frac{1}{2}}(x+y)$	$r^2Y_{23}=(15/2)^{\frac{1}{2}}(xz+yz)$
$rY_{12}=(3/2)^{\frac{1}{2}}(x-y)$	$r^2Y_{24}=(15/2)^{\frac{1}{2}}(xz-yz)$
$rY_{13}=(3)^{\frac{1}{2}}z$	$r^2Y_{25}=(15/4)^{\frac{1}{2}}(x^2-y^2)$
$rY_{14}=(x+y+z)$	$r^2Y_{26}=(5)^{\frac{1}{2}}(xy+yz+zx)$
$rY_{15}=(1/2)^{\frac{1}{2}}(x+y-2z)$	$r^2Y_{27}=(5/2)^{\frac{1}{2}}(xz+yz-2xy)$

2.3 The 4s Wave Function

The procedures required to find the $4s$ wave function in the solid are somewhat different from those described above. The conditions for validity of the tight-binding method no longer hold for the large overlaps characteristic of the $4s$ band in the transition metals. The method, as modified in our work, can nevertheless be used, and gives satisfactory results near the bottom of the $4s$ band. There are two reasons for this. First, by working with the wave function in a single cell of the lattice, we avoid the necessity of summing a slowly convergent series of multicenter integrals. Instead the overlap contribution to the wave function must be evaluated, including the contribution of distant neighbors. This calculation turns out to be practicable. The second reason why our modified tight-binding method can be used even for wave functions with large overlaps is that the wave function is orthogonalized to the core wave functions. This automatically introduces the correct behavior near the nucleus. The tight-binding method under these circumstances is quite similar to the orthogonalized plane wave method,[24] as has been pointed out by Parmenter.[25] The need to orthogonalize valence band wave functions to those of the core has also been stressed by Raimes.[26]

To learn how many terms are required in the expansion of the modified tight-binding wave function for $k\neq 0$, we have made our own empty lattice test. Free-electron wave functions are expanded in spherical harmonics, and the series is truncated in various ways. This work is presented in Appendix A.

Our study of approximations to plane wave expansions shows that good energy values can be obtained with a rather simple approximation, provided we restrict our attention to the lower portion of the band. The form of the wave function we adopt corresponds to that given in Eq. (A5), namely:

$$\Psi_0(\mathbf{k},\mathbf{r})=R_{4s}(r)+\sum_{l,j} d_{0,lj}(\mathbf{k})v_lY_{Lj} +\sum_j d_{0,2j}'(\mathbf{k})r^2Y_{2j}. \tag{15}$$

[24] C. Herring, Phys. Rev. **57**, 1169 (1940).
[25] R. H. Parmenter, Phys. Rev. **86**, 552 (1952).
[26] S. Raimes, Proc. Phys. Soc. (London) **A67**, 52 (1954); P.-O. Löwdin, J. Chem. Phys. **19**, 1579 (1951); see also Appendix B of reference 15 and pp. 70–71 of reference 7.

TABLE III. Matching of truncated atomic contributions to the tight-binding wave function at the centers of the faces of the atomic polyhedron. The spherical harmonics Y_{2j}, which represent the angular dependence of the five $3d$ orbitals, are evaluated at the midpoints of the lines which join the central atom to its 14 closest neighbors at the points $\mathbf{r}_n$. Values associated with next-nearest neighbors are bracketed. The phase factor $\exp(i\mathbf{k}\cdot\mathbf{r}_n)$ is calculated for the point N in the Brillouin zone, where $\mathbf{k}=(\pi/a,\pi/a,0)$. Just inside the cell surface the contribution of the truncated atomic orbital to the tight-binding wave function is $R_{3d}(r)Y_{2j}$, while the contribution at the adjacent point in the next cell is $R_{3d}(r)Y_{2j}\exp(i\mathbf{k}\cdot\mathbf{r}_n)$, where $R_{3d}(r)$ is the atomic radial wave function. Less weight is given to the entries in square brackets, because they correspond to smaller values of R_{3d}. See the text and Wigner and Seitz[a] for further discussion.

		$Y_{2j}(\frac{1}{2}\mathbf{r}_n)$[b]				
$\mathbf{r}_n$	$\exp(i\mathbf{k}\cdot\mathbf{r}_n)$	$\frac{(15)^{\frac{1}{2}}xy}{r^2}$	$\frac{5^{\frac{1}{2}}(2z^2-x^2-y^2)}{2r^2}$	$\frac{(15)^{\frac{1}{2}}(xz+yz)}{2^{\frac{3}{2}}r^2}$	$\frac{(15)^{\frac{1}{2}}(xz-yz)}{2^{\frac{3}{2}}r^2}$	$\frac{(15)^{\frac{1}{2}}(x^2-y^2)}{2r^2}$
$\pm(\frac{1}{2}a,\frac{1}{2}a,\frac{1}{2}a)$	-1	$(5/3)^{\frac{1}{2}}$	0	$(10/3)^{\frac{1}{2}}$	0	0
$\pm(\frac{1}{2}a,\frac{1}{2}a,-\frac{1}{2}a)$	-1	$(5/3)^{\frac{1}{2}}$	0	$-(10/3)^{\frac{1}{2}}$	0	0
$\pm(\frac{1}{2}a,-\frac{1}{2}a,\frac{1}{2}a)$	1	$-(5/3)^{\frac{1}{2}}$	0	0	$(10/3)^{\frac{1}{2}}$	0
$\pm(-\frac{1}{2}a,\frac{1}{2}a,\frac{1}{2}a)$	1	$-(5/3)^{\frac{1}{2}}$	0	0	$-(10/3)^{\frac{1}{2}}$	0
$\pm(0,0,a)$	1	0	$[5^{\frac{1}{2}}]$	0	0	0
$\pm(0,a,0)$	-1	0	$[-(5/4)^{\frac{1}{2}}]$	0	0	$[-(15/4)^{\frac{1}{2}}]$
$\pm(a,0,0)$	-1	0	$[-(5/4)^{\frac{1}{2}}]$	0	0	$[(15/4)^{\frac{1}{2}}]$
$\Sigma\lvert Y_{2j}\rvert\exp(i\mathbf{k}\cdot\mathbf{r}_n)$		0	0	$-(160/3)^{\frac{1}{2}}$	$(160/3)^{\frac{1}{2}}$	$[-(60)^{\frac{1}{2}}]$
$\Sigma Y_{2j}\exp(i\mathbf{k}\cdot\mathbf{r}_n)$		$-(320/3)^{\frac{1}{2}}$	$[(80)^{\frac{1}{2}}]$	0	0	0
Representation[c]		N_1	N_1	N_3	N_2	N_4

[a] See reference 27.
[b] See Table II.
[c] See Table I.

Here l takes on the values 0, 1, 2, 3, 4, with $L=0$ for $l=0$, 2, 4 and $L=1$ for $l=1$, 3. Use of the v_l defined in (11) assures orthogonality to the core wave functions.

Because of the large overlap between neighboring wave functions, the sums over neighbors required to find the $d_{0,lj}$ were carried out through sixth nearest neighbors, and a qualitative correction was made for the contribution from neighbors still further out. This contribution, which may be of some interest in other problems, is developed in Appendix B.

2.4 Interpretation of the Tight-Binding Wave Function

By working with a truncated expansion of the overlap contribution to the tight-binding wave function $\Phi_a(\mathbf{k},\mathbf{r})$, we achieve a simple form which lends itself to visualization and interpretation. This is particularly true when $\mathbf{k}$ is in a direction of high symmetry, because most coefficients in the expansion of Ψ then vanish. Thus we can obtain information about the energy and the charge density of the state by looking at a small number of coefficients.

The two coefficients which give most information about the $3d$ wave function in the solid are $d_{a,00}$, the coefficient of v_0, and $d_{a,2a}$, the coefficient of r^2Y_{2a}, where Y_{2a} is the same spherical harmonic as in the local $3d$ wave function. If $d_{a,00}$ is large in magnitude, the state has a large s-like component. If $d_{a,2a}$ is positive, the overlap portion of the wave function will add to the local wave function, giving a larger amplitude at the surface of the cell and reduced curvature in the wave function. On the other hand a negative value of $d_{a,2a}$ means that the overlap contribution subtracts from the local wave function, increasing the curvature and decreasing the value of the wave function at the surface of the cell.

Our interpretation is based on the tendency of the states with smooth wave functions to have low energies. Thus states with considerable s-like behavior tend to lie near the bottom of the $3d$-$4s$ bands. Of the states with no zero angular momentum terms in the wave function, those with large amplitude at the surface of the atomic cell tend to lie near the bottom of the $3d$ band.

This interpretation is illustrated by Eqs. (13) and (14). Equation (13), representing the wave function of a state at the top of the $3d$ band, has no component with angular momentum lower than two. Also, the amplitude of the wave function goes to zero near the surface of the atomic cell, implying a large curvature in the interior. In contrast, Eq. (14) has components of angular momentum 0 and 1, and also has a relatively large amplitude (but small derivative) at the surface of the cell. It represents a state near the bottom of the $3d$ band.

For the $4s$ band the chief source of information is the coefficient $d_{0,00}$. For states near the bottom of the band, all other coefficients are small and the wave function is almost equal to v_0. As k increases, the overlap contribution to the wave function begins to cancel the local $4s$ wave function, and higher spherical harmonics play an increasingly important role. Under these circumstances a relatively large number of terms in the expansion of the wave function is required. Our approximations are then no longer adequate, and the qualitative features of the wave function cannot be easily characterized.

It is of some interest to compare our interpretation based on the overlap contribution to the wave function

with the model advanced by Wigner and Seitz[27] for predicting the relative positions of energy levels in solids. We apply their model to the states in the $3d$ band whose wave vector is at the endpoint N of the [110] direction in the Brillouin zone. Details are given in Table III. One requirement for a state of low energy is that the contributions of truncated atomic wave functions to the tight-binding wave function join smoothly across the cell boundary.[27] A quantitative measure of the matching at the centers of the faces of the polyhedron is the value of $\sum|Y_{2j}|\exp(i\mathbf{k}\cdot\mathbf{r}_n)$, given in Table III. The larger the algebraic value of this sum, the better the matching of wave functions at the cell boundary, and the lower the predicted energy of the corresponding wave function.

We find that an even more important characteristic of the states of low energy is that they have a component with angular momentum zero. A measure of the s-like component in the tight-binding wave function is $\sum Y_{2j}\exp(i\mathbf{k}\cdot\mathbf{r}_n)$; if the absolute value of this sum is large, the energy of the corresponding state will be low.

If we use these two criteria, and give greater weight to those sums in Table III which arise from nearest neighbors, we see that the energies at the point N in the Brillouin zone should increase as the $3d$ orbitals go through the sequence xy, $xz-yz$, $2z^2-x^2-y^2$, x^2-y^2, $xz+yz$. This order agrees with the calculated results of Sec. 4.2, and is consistent with our interpretation of the overlap contribution to the tight-binding wave function. Similar arguments at other symmetry points of the Brillouin zone also give good agreement with the calculated order of the energy levels.

We have seen that the states of low energy tend to have smooth wave functions, both angularly and radially. The radial dependence is illustrated by Fig. 1, which shows the spherically symmetric part of the charge density of the states at the top and bottom of the $3d$ band at the point N in the Brillouin zone, as given in Eqs. (13) and (14). We see that the state of low energy has a small derivative near $r=r_s$, while the state of high energy has a node near there. For comparison the spherically symmetric part of the overlap charge density of $3d$ electrons on the lattice points is also shown; it lies between the other two curves.

The charge density found by superposing atomic $3d$ electrons corresponds approximately to an average charge density for the entire $3d$ band. If the band is not full, the correlation between smoothness and energy, which we have described above, implies that the charge density will be less sharply peaked than for a full band. Thus x-ray scattering factors for a partially filled $3d$ band will be smaller than one might otherwise expect. This may be relevant to the interpretation of recent measurements of x-ray scattering factors in iron,[28] which find a smaller scattering factor than had been expected, although the effect mentioned here is probably too small to account for the observations.

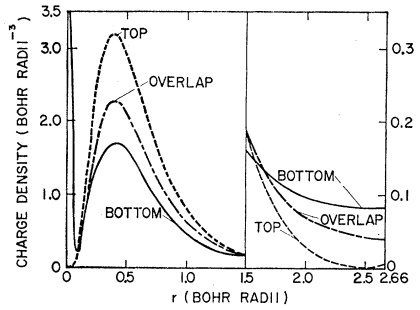

FIG. 1. The spherically symmetric part of the charge density $\rho(r)$ for $3d$ electrons in iron is shown for an atomic sphere radius $r_s=2.66$ Bohr radii. The dashed and solid curves refer, respectively, to the states at the top and at the bottom of the $3d$ band when the wave vector is at the endpoint of a ⟨110⟩ direction in the Brillouin zone. [See Eqs. (13) and (14).] The dot-dash curve gives the spherically symmetric part of the charge density due to overlapping atomic charges, calculated from the adjusted coefficients in Table IV. All charge densities are normalized to 4π over the atomic sphere. Note that the vertical scale has been expanded by a factor of 10 for $r>1.5$.

3. CONSTRUCTING THE POTENTIAL FOR THE SOLID

3.1 Introduction

The atomic polyhedron of the body-centered cubic iron lattice is a truncated octahedron bounded by the planes joining an iron atom to its eight nearest and six next-nearest neighbors. The volume of the polyhedron is $\frac{1}{2}a^3$, corresponding to a sphere of radius $r_s=(3/8\pi)^{\frac{1}{3}}a=0.984745(a/2)$, where a is the lattice constant. At absolute zero, $a=2.860\times10^{-8}$ cm,[29] and $r_s=2.66$ Bohr radii.

In much of the work which follows we shall replace the atomic polyhedron by a sphere of radius r_s. This is not a bad approximation, since the inscribed sphere and circumscribed sphere of the atomic polyhedron have radii $0.88r_s$ and $1.14r_s$, respectively. Another measure of the small deviation of the polyhedron from spherical shape is the fact that only about 8% of its volume lies outside the sphere of radius r_s. We therefore have good reason to expect that for most purposes replacing the polyhedron by the sphere will be a valid approximation.

We find a first approximation to the charge density in the solid by superposing the charge densities of free

[27] E. P. Wigner and F. Seitz, in *Solid-State Physics*, edited by F. Seitz and D. Turnbull (Academic Press, Inc., New York, 1955), Vol. I, p. 97.

[28] R. J. Weiss and J. J. DeMarco, Revs. Modern Phys. **30**, 59 (1958); Phys. Rev. Letters **2**, 148 (1959). See also B. W. Batterman, Phys. Rev. Letters **2**, 47 (1959); Hume-Rothery, Brown, Forsyth, and Taylor, Phil. Mag. **3**, 1466 (1958); R. D. Deslattes, Phys. Rev. **110**, 1471 (1958); B. W. Batterman, Phys. Rev. **115**, 81 (1959).

[29] W. B. Pearson, *A Handbook of Lattice Spacings and Structures of Metals and Alloys* (Pergamon Press, Inc., New York, 1958), pp. 625–627.

atoms located at the lattice points. In doing this, care must be taken to make the charge density self-consistent, i.e., to make it correspond as closely as possible to the charge density of the states actually occupied in the solid.

Simple superposition of the charge densities of free iron atoms in their lowest configuration will not lead to a self-consistent potential. This was shown in a trial calculation preliminary to the present one,[15] and also in Callaway's work.[30] Both of these calculations were based on the charge density calculated for the $3d^64s^2$ configuration of atomic iron by Manning and Goldberg[31] using the self-consistent field method without exchange. In both cases the $3d$ band was found to be completely below the $4s$ band in energy, which would imply that the configuration in the solid was $3d^8$, inconsistent with the starting configuration $3d^64s^2$. Both calculations also found the $3d$ band to be about 0.1 ry wide, which is narrower than the widths suggested by x-ray emission measurements.[32]

These considerations led to self-consistent field calculations for the $3d^74s$ and $3d^8$ configurations of atomic iron[15,20] which showed that there are substantial changes in the charge distribution and in the energy of $3d$ electrons as the configuration changes. As electrons are transferred from the $4s$ to the $3d$ band the screening of the nuclear charge increases. This weakens the Coulomb attraction of the nucleus, and results in an increase in the energy of the $3d$ states and in a more diffuse $3d$ charge distribution. The $4s$ electrons are less strongly affected.

Availability of self-consistent field calculations for three configurations of atomic iron makes possible construction of a more reasonable charge density and potential for the solid. In the present calculation the charge density at each lattice point is considered to be contributed by n_{4s} $4s$ electrons and n_{3d} $3d$ electrons, where $n_{4s}+n_{3d}=8$ is the total number of valence electrons in iron. We leave n_{4s} as a parameter in the calculation, and choose its value so as to maximize the cohesive energy of the solid. We fall short of a completely consistent procedure, however, in that we use the atomic $3d$ and $4s$ wave functions calculated for the $3d^74s$ configuration. That choice is made in the interest of simplicity, but turns out to agree with the configuration our calculation predicts for the solid.

[30] J. Callaway, Phys. Rev. **99**, 500 (1955).
[31] M. F. Manning and L. Goldberg, Phys. Rev. **53**, 662 (1938).
[32] E. M. Gyorgy and G. G. Harvey, Phys. Rev. **93**, 365 (1954), estimate that the $3d$ band of iron is 2.2 ev (0.16 ry) wide. Their interpretation is questioned by Skinner, Bullen, and Johnston, Phil. Mag. **45**, 1070 (1954), who find the band width in iron to be about 5 or 6 ev. Dr. Ronald Newburgh (private communication) points out that earlier measurements were generally made on films evaporated under relatively poor vacuum conditions. Experiments done by him and G. G. Harvey on carefully cleaned solid specimens of copper and nickel give emission bands about twice as wide as those found by earlier workers, with two clearly resolved peaks in each band. The author is grateful to Dr. Newburgh for making this information available prior to publication.

Because of the different approximations required, we discuss the $3d$ and $4s$ contributions to the total charge density in the solid separately.

3.2 $3d$ Electrons

In an atomic sphere we divide the charge density per $3d$ electron into the part contributed by the electron in the sphere and the additional charge density, or overlap charge, of $3d$ electrons at the remaining lattice points $\mathbf{r}_n$. The overlap charge density, ρ', is given by:

$$\rho_{3d}'(\mathbf{r})=\sum_n{}'[R_{3d}(\mathbf{r}-\mathbf{r}_n)]^2, \tag{16}$$

where $\mathbf{r}$ is a point in the central cell, R_{3d} is the radial wave function (normalized to give $\int R^2r^2dr=1$) of a $3d$ electron in the $3d^74s$ configuration,[20] and the primed sum over $\mathbf{r}_n$ excludes the origin.

We have evaluated Eq. (16), for a body-centered cubic lattice, at the origin of the central cell and at 5 points in each of the three symmetry directions $\langle 001\rangle$, $\langle 111\rangle$, and $\langle 110\rangle$. The contribution of the closest 26 neighboring atoms was found exactly, and the effect of more distant neighbors was estimated. These calculations were made using $r_s=2.30$, 2.66, and 3.10.

The charge density contributed by neighboring atoms can be expanded in cubic harmonics:

$$\rho_{3d}'(\mathbf{r})=\rho_0(r)+\rho_4(r)G+\rho_6(r)I, \tag{17}$$

where G and I are cubic harmonics[33] of order 4 and 6:

$$G=5(x^4+y^4+z^4)r^{-4}-3, \tag{18}$$

$$I=231[x^2y^2z^2r^{-6}+(G/110)-(1/105)]. \tag{19}$$

Their normalizations on the unit sphere are: $\int G^2d\Omega=64\pi/21$, and $\int I^2d\Omega=128\pi/13$.

From the values of ρ' found in the three symmetry directions, we find the coefficients of the spherical harmonics in (17) using:

$$\begin{aligned}\rho_0&=(10\rho_{001}+9\rho_{111}+16\rho_{110})/35,\\ \rho_4&=(35\rho_{001}-27\rho_{111}-8\rho_{110})/110,\\ \rho_6&=(3\rho_{001}+9\rho_{111}-12\rho_{110})/77,\end{aligned} \tag{20}$$

where, for example, ρ_{110} is the value of $\rho'(\mathbf{r})$ at a point in a $\langle 110\rangle$ direction, and all expressions refer to the same radial distance r from the origin of the cell. The anisotropy of the charge density is greatest near the surface of the atomic sphere. For example $\rho_{001}=0.022$, $\rho_{111}=0.058$, and $\rho_{110}=0.023$, all at the surface of the atomic sphere for $r_s=2.66$. To these overlap charge densities must be added the local charge density, $[R_{3d}(2.66)]^2=0.015$. These values can be compared with the charge density of a uniform charge distribution, which has the value 0.159 for $r_s=2.66$.

We have expanded the coefficients of the cubic

[33] F. C. Von der Lage and H. A. Bethe, Phys. Rev. **71**, 612 (1947).

TABLE IV. Coefficients of the power series expansion of the charge density produced in an atomic sphere of body-centered cubic iron by overlap of spherically symmetric $3d$ electron charge distributions on all other lattice points. Charge is given in units of the electron charge and distance in units of the Bohr radius. $Z(r)$ is the charge within a sphere of radius r; see Eqs. (17)–(21) for the definition of the $c_{n,p}$. The second set of zero-order coefficients has been adjusted to give unit charge in the sphere of radius r_s.

	r_s: 2.30	2.66	3.10
$c_{0,0}$	1.46×10^{-2}	5.14×10^{-3}	1.52×10^{-3}
$c_{0,2}$	4.58×10^{-3}	1.55×10^{-3}	4.34×10^{-4}
$c_{0,4}$	5.54×10^{-4}	1.60×10^{-4}	4.28×10^{-5}
$c_{0,6}$	4.2×10^{-5}	1.39×10^{-5}	3.2×10^{-6}
$c_{0,10}$	1×10^{-6}	1.5×10^{-7}	2×10^{-8}
$Z_{\text{overlap}}(r_s)$	0.158	0.109	0.070
$c_{4,4}$	-2.9×10^{-4}	-8.1×10^{-5}	-2.0×10^{-5}
$c_{4,6}$	-1.2×10^{-5}	-5.9×10^{-6}	-0.8×10^{-6}
$c_{4,8}$	-7.2×10^{-6}	-1.1×10^{-6}	-2.6×10^{-7}
$c_{6,6}$	2.3×10^{-5}	5.4×10^{-6}	1.1×10^{-6}
$c_{6,8}$	4.3×10^{-6}	8.5×10^{-7}	1.3×10^{-7}
adjusted			
$c_{0,0}$	1.46×10^{-2}	5.14×10^{-3}	1.52×10^{-3}
$c_{0,2}$	4.58×10^{-3}	1.55×10^{-3}	4.34×10^{-4}
$c_{0,4}$	5.05×10^{-4}	1.60×10^{-4}	4.28×10^{-5}
$c_{0,6}$	0	4.4×10^{-7}	4.4×10^{-7}
$Z_{\text{overlap}}(r_s)$	0.143	0.095	0.058

harmonics in Eq. (17) in powers of r:

$$\rho_n=\sum_p c_{n,p}r^p, \quad p=n, n+2, \cdots. \tag{21}$$

These coefficients are listed in Table IV for each of the three values of r_s.

The total charge in the atomic sphere surrounding a lattice point can be found from the values of Table IV by integrating the spherically symmetric part of the charge density. The fraction of the charge of a $3d$ electron from the $3d^74s$ configuration within a sphere of radius 2.66 is 0.905.[20] If we use values for $r_s=2.66$ from Table IV, we find an overlap contribution of 0.109. Thus the charge in the unit sphere around a lattice point is found to be 1.014, even though the charge density was constructed by putting one $3d$ electron at each lattice point. This discrepancy arises because both the charge density and the atomic polyhedron lack spherical symmetry. The atomic sphere lies outside the polyhedron on the line joining nearest neighbors, where the charge density is large, and lies inside the polyhedron in regions of lower charge density. Thus the uncorrected values from Table IV lead to electronic charge in the unit sphere in excess of the charge on the positive ion located there.

We have corrected for the apparent deviation from charge neutrality in the atomic sphere by using a spherically symmetric $3d$ charge density which is adjusted to give unit charge in the sphere. Strictly speaking, any change in the originally calculated charge density should be confined to the region outside the inscribed sphere of the atomic polyhedron. We have instead reduced the coefficient of the highest power of r in the expansion of ρ_0. This also confines the correction principally to the outer portion of the sphere. The adjusted coefficients, and the corresponding values of the overlap charge inside the atomic sphere, are given in the last five lines of Table IV.

The potential energy of an electron interacting with the adjusted spherically symmetric charge distribution in the atomic sphere is $2Y_{3d}(r)/r$, where

$$2Y_{3d}(r)=2Y_{3d,\,\text{atom}}(r)+Ar-2\sum_p(p+2)^{-1}(p+3)^{-1}c_{0,p}r^{p+3}, \tag{22}$$

and

$$A=[2\sum_p(p+2)^{-1}c_{0,p}r_s^{p+2}]-r_s^{-1}[2Y_{3d,\,\text{atom}}(r_s)-2Z_{3d,\,\text{atom}}(r_s)]. \tag{23}$$

$Z(r)$ is the charge within a sphere of radius r, and $2Y(r)/r$ is the potential at point r, in both cases for a single electron per atom.[34]

This completes the determination of the charge density and potential produced in the solid by one $3d$ electron per atom. The total potential is constructed in Sec. 3.4.

Equation (16), with which the foregoing considerations began, assumes that each $3d$ electron has a spherically symmetric charge distribution about its own nucleus. This leads to correct results if the $3d$ band is completely filled; otherwise, the angular dependence of the individual $3d$ space orbitals will not be completely canceled. This effect, like other departures from spherical symmetry, is neglected here. The $3d$ potential we have constructed is not completely self-consistent, i.e., it does not correspond exactly to the potential of the states actually occupied in the solid. We correct for the departure from self-consistency in Sec. 5 where we calculate the cohesive energy.

3.3 4s Electrons

The procedure required to find the charge density and potential per $4s$ electron in the solid is considerably different from the one we have described for $3d$ electrons. Only 0.245 of the charge of a $4s$ electron in the $3d^74s$ configuration of atomic iron is contained in a sphere of radius 2.66, while 0.905 of the charge of a $3d$ electron is inside this sphere. Thus the charge density in the solid would be almost constant if individual $4s$ electron charge densities were superposed. We use the $4s$ wave functions of the solid and include the effects of orthogonalization to the core before finding the potential, since this orthogonalization is much more important for $4s$ electrons than for $3d$ electrons.

We have calculated the spherically symmetric part of the charge density for several states in the $4s$ band, using the wave functions described in Sec. 2.3. These charge distributions do not depend strongly on the energy of the state, and we make only a small error in neglecting the dependence of the shape of the charge

[34] The atomic values of Z and $2Y$ are those for the $3d^74s$ configuration. See reference 20 for further details, particularly footnote 11 therein.

distribution on the number of $4s$ electrons per atom. We use the charge density for 0.6 $4s$ electrons per atom, normalized to give unit charge in the atomic sphere, as the charge density per $4s$ electron. The potential per $4s$ electron, $2Y_{4s}(r)/r$, is easily found from this charge density. Here, as for $3d$ electrons, the calculation was carried out for $r_s=2.30$, 2.66, and 3.10.

3.4 The Total Potential in the Atomic Sphere

The potential field felt by a valence electron of iron is, in our approximation, the potential of the ion core plus the potential of the remaining 7 valence electrons. We assume that on the average there are n_{4s} $4s$ electrons and $n_{3d}=(8-n_{4s})$ $3d$ electrons in the atomic sphere. There remains some arbitrariness about the configuration in any particular atomic cell.[35] We assume that a fraction n_{4s} of the atomic cells is in the $3d^7 4s$ configuration, and a fraction $1-n_{4s}$ is in the $3d^8$ configuration. This has the advantage that the calculation can be readily carried out in parallel for the solid and for the same mixture of configurations in the free atom. It limits the range of validity to values of n_{4s} between 0 and 1.

With the foregoing approximation the potential field $V_{4s}(r)$ in which a $4s$ electron moves is independent of n_{4s}. The potential $V_{3d}(r)$ seen by a $3d$ electron is an average over the two configurations. We find:

$$V_{4s}(r)=r^{-1}(-52+2Y_{\text{core}}+14Y_{3d}), \tag{24}$$

$$V_{3d}(r)=r^{-1}\{-52+2Y_{\text{core}}+n_{3d}^{-1}\times[(112-28n_{4s})Y_{3d}+14n_{4s}Y_{4s}]\}. \tag{25}$$

Here $2Y_{3d}$ and $2Y_{4s}$ are the functions of r found in Secs. 3.2 and 3.3, and $2Y_{\text{core}}$ is the corresponding function for the 18 core electrons as used in the self-consistent field for the $3d^7 4s$ configuration of atomic iron.[20] The potentials in Eqs. (24) and (25) were calculated for $r_s=2.30$, 2.66, and 3.10. In all cases $V(r_s)=-2/r_s$, and $rV(r)\to-52$ as $r\to 0$. We have made some very small adjustments in the potentials of the $3s$ and $3p$ electrons of the core, since not quite all of their charge is contained within a sphere of radius 2.30 Bohr radii. This has a negligible effect on the cohesive energy, but may have a slight effect on the compressibility.

Use of n_{4s} as a parameter, whose value is to be chosen to maximize the cohesive energy, has only qualitative validity, since the full symmetry of the rotation group is lost in the solid and quantum numbers appropriate for free atoms can no longer be used. Thus the $3d$ and $4s$ bands are mixed in the solid. It is nevertheless useful to assume that the charge density in the unit cell is contributed by a certain number of $3d$ and $4s$ electrons per atom.

[35] J. H. Van Vleck, Revs. Modern Phys. **25**, 220 (1953).

4. ONE-ELECTRON ENERGIES

4.1 The Boundary Correction

When the one-electron energy is evaluated in a single cell of the lattice, as in our work, some care must be taken with the kinetic energy operator T. Normally

$$T=-(\hbar^2/2m)\Delta=-(\hbar^2/2m)\times[(\partial^2/\partial x^2)+(\partial^2/\partial y^2)+(\partial^2/\partial z^2)].$$

Application of Green's theorem in a volume having a finite boundary S gives:

$$\int[f^*\Delta g-(\Delta f)^*g]d\tau=\int[f^*\nabla g-(\nabla f)^*g]\cdot d\mathbf{S}, \tag{26}$$

which will not vanish in general. Thus the Laplacian, and with it the kinetic energy, will not be Hermitian when applied to an arbitrary function in a finite volume. From (26) it is clear that the modified kinetic energy operator:

$$T=-(\hbar^2/2m)\Delta+(\hbar^2/2m)\delta(\mathbf{n})(\partial/\partial n) \tag{27}$$

is Hermitian. The derivative in the second term of (27) is along the outward normal, and the delta function indicates that it is to be evaluated on the surface S. This additional term in the kinetic energy is called the boundary correction,[27,15] and has been used for many years. It appeared in early work on sodium,[36] and has been applied in several forms of the cellular method.[37] Kohn's[38] variational principle for solids includes the boundary correction and also incorporates the Bloch periodicity requirements.

An interesting qualitative result deduced from the surface correction is that the lowest energy of an s-band in a solid will first decrease as the lattice constant si reduced from infinity, but will then rise again before the atomic wave function reaches its outermost maximum, where the boundary correction vanishes. An exception is a band based on $1s$ wave functions, as in metallic hydrogen[39] or the analogous system of a regular array of impurities in a semiconductor.[40] In these cases the derivative of the wave function does not change sign, and the energy of the bottom of the band continues to decrease as the lattice constant is decreased.

4.2 One-Electron Energy Results

The energies of states in the $3d$ and $4s$ bands are given by:

$$E_a(\mathbf{k})=(\Psi_a|H|\Psi_a)/(\Psi_a|\Psi_a), \tag{28}$$

[36] E. Wigner and F. Seitz, Phys. Rev. **46**, 509 (1934), Appendix I. See also p. 363 of reference 16.

[37] D. J. Howarth and H. Jones, Proc. Phys. Soc. (London) **A65**, 355 (1952); M. M. Saffren and J. C. Slater, Phys. Rev. **92**, 1126 (1953); D. P. Jenkins and L. Pincherle, Phil. Mag. **45**, 93 (1954).

[38] W. Kohn, Phys. Rev. **87**, 472 (1952).

[39] E. Wigner and H. B. Huntington, J. Chem. Phys. **3**, 764 (1935); Kronig, De Boer, and Korringa, Physica **12**, 245 (1946); N. H. March, Physica **22**, 311 (1956).

[40] F. Stern and R. M. Talley, Phys. Rev. **100**, 1638 (1955).

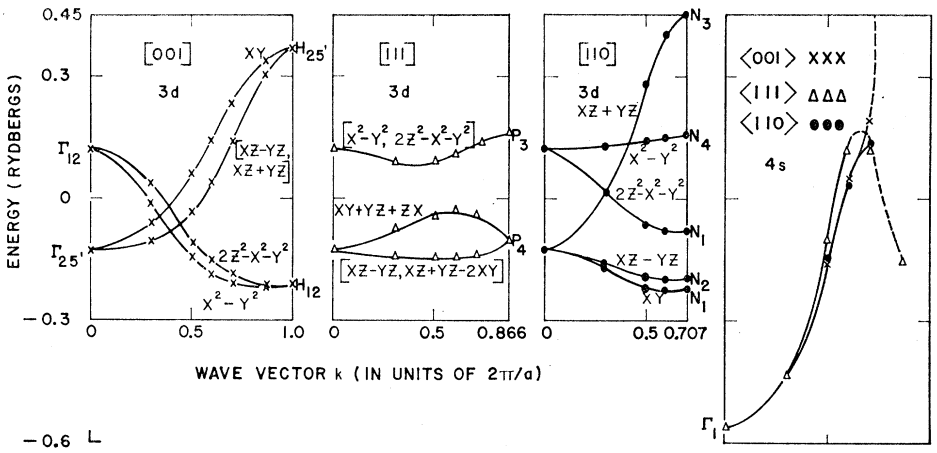

FIG. 2. Calculated band structure of body-centered cubic iron in the configuration $3d^7 4s$, for $r_s = 2.66$. The $3d$ bands are shown in the three directions of high symmetry, and the dominant angular dependence of the wave function is indicated for each band. Brackets indicate degenerate states. The dashed portions of the $4s$ band are of doubtful accuracy. The symmetry character of the states at the center and on the surface of the Brillouin zone is indicated, in the notation of reference 22. Note that the off-diagonal matrix elements of the Hamiltonian connecting states of the same symmetry have not been removed. Energies were calculated for the following wave vectors: 0, 0.3, 0.5, 0.6, 0.707, 0.866, and 1.0, in units of $2\pi/a$, where a is the lattice constant. If these values were corrected for the departure of the potential from self-consistency, the $3d$ bands would be lowered by about 0.15 ry, but the $4s$ band would be changed very little.

where the modified tight-binding wave function Ψ_a has the form given in Eq. (12) or (15). The Hamiltonian H contains the kinetic energy operator of Eq. (27) and the potential energy of Eq. (24) or (25). Many terms enter in the evaluation of (28), but the work is straightforward and details are not given here.

Twelve complete band structures were found for body-centered cubic iron, taking $r_s = 2.30$, 2.66, and 3.10, and $n_{4s} = 0.3$, 0.6, 0.9, and 1.0. In each case the energy was found for 16 nonequivalent points of high symmetry in the Brillouin zone. In Fig. 2 we show the band structure for $r_s = 2.66$ and $n_{4s} = 1.0$, the parameters closest to those of the equilibrium configuration of the solid. Off-diagonal elements of the Hamiltonian have not been removed, and the crossings of the $3d$ and $4s$ bands indicated in Fig. 2 are spurious. We have shown by dashed lines a portion of the $4s$ band near the surface of the Brillouin zone, where our approximations are no longer valid and the energy values are uncertain.

The qualitative features of the band structure are comparable with those found by Callaway[30] using the orthogonalized plane wave method, by Wood[41] using the augmented plane wave method, and by Manning[42] using the cellular method. No detailed comparison of the four calculations is possible, since different potentials were used. Our work, like that of Wood and of Manning, shows that the top of the $3d$ band belongs to the representation N_3, whereas Callaway indicates N_4. We give the following comparison of results for the over-all width of the $3d$ band:

$$\begin{aligned} &\text{Callaway}^{30}\ 0.12\ \text{ry}, \quad \text{Wood}^{41}\ 0.46\ \text{ry}, 0.88\ \text{ry}, \\ &\text{Manning}^{42}\ 0.62\ \text{ry}, \quad \text{Present work}\ 0.68\ \text{ry}. \end{aligned} \tag{29}$$

The two band widths found by Wood are for different potentials, the first corresponding to the one used by Manning, and the second corresponding to the rather diffuse charge density suggested by x-ray scattering results.[28] Callaway used a potential based on the $3d^6 4s^2$ configuration of the free atom, with an effective exchange potential.

Another interesting quantity is the width of the occupied portion of the $3d$ band. To find the position of the Fermi level for $r_s = 2.66$, we have plotted in Fig. 3 the apparent Fermi level in the $3d$ and $4s$ bands for various configurations. To do this we assign weights to each of the sixteen points in the Brillouin zone for

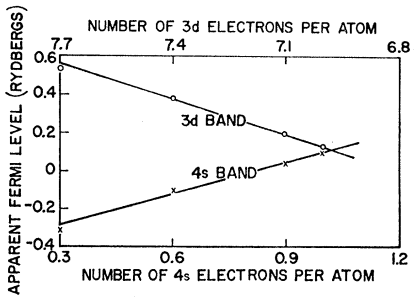

FIG. 3. Apparent position of the Fermi level in the $3d$ and $4s$ bands for several configurations. The stable configuration has the Fermi level at the same energy in both bands, and corresponds to 1.0 $4s$ electrons and 7.0 $3d$ electrons per atom. The energy values used here have not been corrected for the departure of the potential from self-consistency.

[41] J. H. Wood, Solid-State and Molecular Theory Group, Massachusetts Institute of Technology, Quarterly Progress Reports No. 31, January 15, 1959, and No. 28, April 15, 1958 (unpublished).

[42] M. F. Manning, Phys. Rev. **63**, 190 (1943).

which energy values were found, such that the sum of these weights corresponds to two electrons per atom. The sum of the weights of all states whose energy is less than or equal to the apparent Fermi level gives the band occupation. The stable configuration of the crystal for a given lattice constant is the one for which the apparent Fermi levels in the $3d$ and $4s$ bands are equal. When $r_s=2.66$ we find the stable configuration to be $3d^{7.0}4s^{1.0}$, and the energy of the Fermi level to be 0.11 ry. A similar procedure for $r_s=2.30$ and 3.10 gives the same configuration. The width of the occupied portion of the band is 0.33 ry for $r_s=2.66$. X-ray emission spectra of iron[32] do not give a reliable band width for comparison with the calculated result.

We have not corrected the individual one-electron energies for the difference between the potential which corresponds to the states occupied in the solid and the potential which was used in the Hamiltonian [Eq. (24) or (25)]. The actual charge density turns out to be somewhat more diffuse than the one which was used in Sec. 3, and as a result the corrected one-electron energies in the $3d$ band will be about 0.15 ry lower than the values shown in Fig. 2. The $4s$ band is not greatly affected. This correction for the departure of the potential from self-consistency is made in Sec. 5 where we find the total energy of the solid. If it were made in the determination of the Fermi level, the calculated equilibrium configuration of the solid would be about $3d^{7.1}4s^{0.9}$.

The density of states has been calculated from the one-electron energies of Fig. 2. At the Fermi level we find about 25 $3d$ electrons per atom per Rydberg, and about 3 $4s$ electrons per atom-ry. The density of states deduced from the experimental electronic specific heat of body-centered cubic iron[43] is 29 electrons per atom-ry. We cannot compare the experimental result with our calculation because the experiment is carried out on ferromagnetic iron, while the calculation assumes a singlet spin state. Our density of states is not very accurate, partly because of the small number of points in our band structure, and partly because of the approximations used to calculate the density of states. It does, however, have the two-humped shape generally assumed for transition elements.[44] We find one peak near the bottom of the $3d$ band, with a second peak just above the Fermi level. Our calculation also gives a region at the top of the $3d$ band with a very small density of states, containing about one of the 10 $3d$ electrons per atom. This region might well be modified by interaction with higher bands.

We find the effective mass at the bottom of the $4s$ band to be $0.85m$ for $r_s=2.66$.

[43] G. Duyckaerts, Physica **6**, 401 (1939); W. H. Keesom and B. Kurrelmeyer, Physica **6**, 364, 633 (1939).

[44] J. E. Goldman, Revs. Modern Phys. **25**, 108 (1953), Sec. II; Wei, Cheng, and Beck, Phys. Rev. Letters **2**, 95 (1959).

5. COHESIVE ENERGY OF THE SOLID

Having found the one-electron energies in the valence bands of metallic iron, we are now in a position to find the total energy of the solid and compare it with the energy of the ground state of the free atom to obtain the cohesive energy. We consider the 18 electrons of the core in iron to be unchanged during the transition from atom to metal, and need not take the internal energy of the core into account.

The total energy of the solid is not given simply by the sum of one-electron energies, since that sum counts interactions between valence electrons too often. The total energy per atomic cell for the configuration having n_{4s} $4s$ electrons and $(8-n_{4s})$ $3d$ electrons is calculated on the assumption that a fraction n_{4s} of the cells is in the $3d^64s$ configuration, and that the remaining fraction, $1-n_{4s}$, is in the $3d^8$ configuration. We neglect all Slater integrals other than F^0,[45] and find for the total energy per cell in the solid:

$$E(\text{solid,total})=\sum E_a(\mathbf{k})-28F_{dd}-7n_{4s}(F_{sd}-F_{dd}). \quad (30)$$

Here the one-electron energies $E_a(\mathbf{k})$ are to be summed over all occupied states in the valence band, each weighted in such a way that the sum of the weights equals the number of valence electrons per atom, which is 8 for iron. Subscript d stands for $3d$, and s stands for $4s$. The F_{ab} are average Coulomb interaction energies between electrons a and b in the solid, i.e.:

$$F_{ab}=F_{ba}=\int_0^{r_s} 2Y_a(r)\rho_b(r)rdr, \quad (31)$$

where $\rho_b(r)$ is the spherically symmetric part of the charge density per electron averaged over all occupied states in the b-band and normalized to 4π in the sphere of radius r_s, and $2Y_a(r)/r$ is the potential associated with the charge density $\rho_a(r)$. Thus F_{ab} is a function of r_s, and may also depend on the configuration in the solid.

A first approximation to F_{sd} and F_{dd} can be calculated from the charge densities and potentials described in Secs. 3.2 and 3.3. These values are called $F_{dd,0}$ and $F_{sd,0}$, and are given in Table V, which lists all the quantities used in finding the total energy. As one might suspect from the discussion of Sec. 3.4, and from Fig. 1, F_{dd} is rather sensitive to the occupation of the $3d$ band. It tends to increase as the band occupation rises, because the states at the top of the $3d$ band have a more sharply peaked charge distribution than do those at the bottom. For this reason we determined the value of F_{dd} for each configuration for which the total energy was evaluated. These results are also given in Table V. The dependence of F_{sd} on band occupation is not as great as for F_{dd}, and F_{sd} enters in the total energy with

[45] The Slater integrals are defined by E. U. Condon and G. H. Shortley, *The Theory of Atomic Spectra* (Cambridge University Press, London, 1935), Sec. 8[6], or in reference 20. By "higher Slater integrals" we mean all Slater integrals other than F^0.

TABLE V. Quantities used to find the total energy of the solid and of the free iron atom. F_{ab} is the average energy of interaction between an electron of type a and one of type b defined in Eq. (31); subscript d stands for a $3d$ electron, s for a $4s$ electron. ΣE_a and E(total) are defined in Eq. (30). The number of $4s$ electrons per atom is n_{4s}. All values have been rounded to three decimals and are in Rydbergs, except that r_s is given in units of the Bohr radius. $F_{sd,0}$ and $F_{dd,0}$ are calculated from the charge densities and potentials of Sec. 3, while the remaining values of F_{dd} are found for the charge density corresponding to the occupied states in the indicated configuration.

			$n_{4s}=0.3$			$n_{4s}=0.6$			$n_{4s}=0.9$			$n_{4s}=1.0$		
r_s	$F_{sd,0}$	$F_{dd,0}$	F_{dd}	ΣE_a	E(tot)	F_{dd}	ΣE_a	E(tot)	F_{dd}	ΣE_a	E(tot)	F_{dd}	ΣE_a	E(tot)
2.30	1.092	1.484	1.465	3.099	−37.138	1.455	1.861	−37.352	1.443	0.686	−37.499	1.438	0.313	−37.533
2.66	0.956	1.434	1.402	1.082	−37.249	1.396	−0.239	−37.470	1.385	−1.537	−37.616	1.381	−1.953	−37.652
3.10	0.839	1.402	1.372	0.230	−37.058	1.365	−1.269	−37.274	1.357	−2.742	−37.464	1.354	−3.213	−37.511
∞	0.609[a]	1.370[a]			−36.633			−36.755			−36.878			−36.919

[a] These values are taken from the $3d^74s$ configuration (reference 20).

a relatively small multiplier. Therefore, we have not determined the dependence of F_{sd} on band occupation, and use the value $F_{sd,0}$ found from the charge densities of Sec. 3. The values of $\sum E_a$ given in Table V, like the values of F_{dd}, have been corrected to correspond to the actual charge density in the indicated configuration.

The cohesive energy of the solid is the difference between the energy of the solid, taken to be in singlet state in our work, and the energy of the atom in its ground state, $^5D_4$. We find this difference in two steps. The first step, shown in Table V, compares the energy of the solid with the energy of the atom in an average singlet state of the same configuration. We neglect all higher Slater integrals,[45] both between pairs of valence electrons and between valence electrons and the core. These integrals will contribute approximately equal amounts to the energy of the solid and of the atom in the reference state. Thus some sources of error are reduced when we compare the energy of the atom and of the solid in the same state.

When higher Slater integrals are dropped, the energy of the atom in a configuration with n_{4s} $4s$ electrons is:

$$E(\text{total,atom})=n_{4s}E(\text{atom},3d^74s)+(1-n_{4s})E(\text{atom},3d^8), \quad (32)$$

where, for example,[46]

$$E(\text{atom},3d^8)=8E_{3d}(3d^8)-28F_{dd}(3d^8),$$

and the energy for the $3d^74s$ configuration has a similar form. The numerical values $E(\text{atom},3d^74s)=-36.919$ and $E(\text{atom},3d^8)=-36.510$ are found using the results of atomic self-consistent field calculations without exchange.[20] Values of Eq. (32) for the various configurations are listed in Table V, where $r_s=\infty$ refers to the free atom.

The second step in finding the cohesive energy is to calculate the difference between the energy of the average singlet state of the reference configuration and the energy of the atomic ground state. This difference, taken largely from experiment,[47] is 0.303 ry for $3d^74s$ and 0.429 ry for $3d^8$, and is interpolated linearly for intermediate configurations. Combining the two steps, we find:

$$-E(\text{cohesive})=E(\text{solid,total})-E(\text{atom,total})+0.429-0.126n_{4s}. \quad (33)$$

We evaluate (33) for each value of n_{4s} and r_s, using the entries of Table V, and list the results in Table VI.

For each value of r_s, a least-squares-fitted parabola can be passed through the four values of Eq. (33) given in Table VI. The minimum of this parabola gives the energy of the solid relative to the energy of the free atom, and the number of electrons per atom, at the given value of r_s. The energy and the value of n_{4s} found in this way are shown in the last two columns of Table VI. Note that the scatter of points leads to a small inconsistency for $r_s=2.66$, where the minimum found by least squares is higher than one of the calculated points. More serious is the situation for $r_s=3.10$, where the minimum energy of the solid falls well outside the range of validity of our approximation, which is good only for $0\leq n_{4s}\leq 1$.

TABLE VI. Energy per atom of metallic iron, relative to the energy of the ground state, $^5D_4$, of the free iron atom. All energies are in Rydbergs. The last two columns give the minimum energy and the corresponding number of $4s$ electrons per atom, as found from a parabolic least-squares fit at each value of the unit sphere radius r_s.

r_s	n_{4s}: 0.3	0.6	0.9	1.0	$E_{\min}$	n_{4s}
2.30	−0.114	−0.242	−0.304	−0.310	−0.310	1.03
2.66	−0.225	−0.361	−0.421	−0.429	−0.428	1.02
3.10	−0.035	−0.164	−0.270	−0.289	−0.359	1.59

[46] We use the $3d$ wave function of the $3d^8$ configuration to find $E(\text{atom},3d^8)$. Had we used the $3d$ wave function of the $3d^74s$ configuration, on the ground that wave functions from this configuration were used throughout the calculation for the solid, we would have $E(\text{atom},3d^8)=-36.233$. This would increase the calculated binding energy of the solid by about 0.1 ry, and would reduce to about 0.7 the value of n_{4s} which maximizes the cohesive energy.

[47] The term value for the average singlet state of $3d^74s$ is found from the experimental values listed in Table IV of reference 20, except that the higher ^1D term value, which has not been measured, is taken from the least-squares fit in that table. The average singlet term value for $3d^8$ is based on the calculated values for Racah's parameters B and C, also listed in Table IV of reference 20, together with the observed ^3F term value of $3d^8$. The calculated singlet term values of reference 20 are higher than the observed values, especially for $3d^8$. Use of the calculated values would lower the calculated cohesive energy of metallic iron by about 0.2 ry, and would increase the value of n_{4s} which maximizes the cohesive energy by about 0.3.

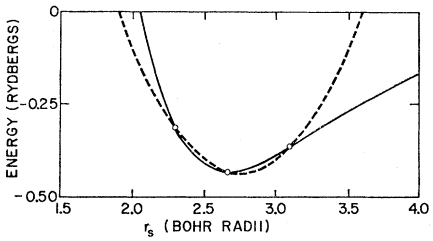

FIG. 4. Two ways of fitting a smooth curve to the calculated values of the energy of the solid. The dashed curve is the parabola of Eq. (34), and the solid curve is the Morse function of Eq. (35). The zero level is the energy of a free iron atom in its ground state.

The minimum energy values of Table VI permit us to find the cohesive energy, equilibrium lattice constant, and compressibility of the solid. The parabola through the minimum energy values is:

$$E=-0.433+0.606(r_s-2.75)^2, \qquad (34)$$

where the energy is in Rydbergs and r_s is in Bohr radii. The energy of the solid relative to that of the free atom goes to zero as r_s increases. A parabola is thus a poor curve for fitting the calculated energy points. We have chosen, in preference to (34), an expression which goes to zero as r_s becomes infinite. This is a Morse function which, for the values in Table VI, has the form:

$$E=0.428\{\exp[-2.34(r_s-2.66)] -2\exp[-1.17(r_s-2.66)]\}. \qquad (35)$$

The energy curves of Eqs. (34) and (35) are shown in Fig. 4.

From both Eq. (35) and Eq. (34) we find the cohesive energy of the solid to be 0.43 ry per atom, as compared to the experimental value 0.32 ry.[48] To estimate the errors in the theoretical value we must consider both the arbitrary choices made in our work and the effects which were not included at all. The uncertainty of the calculated cohesive energy is estimated to be 0.2 ry, and the value of n_{4s} for which the cohesive energy is a maximum is in doubt by about 0.3. The agreement of our calculated energy with experiment gives encouraging evidence that cohesive energy calculations for many-electrons metals like the transition metals are practicable.

Some additional basis for confidence in our result comes from the equilibrium value of r_s predicted by our calculation. The value $r_s=2.66$ given by (35) is in exact agreement with experiment, and the value 2.75 given by (34) is quite close. Because of the arbitrariness of fitting a curve to only three points, we can say only that the predicted lattice constant is within about 0.1 Bohr radius of the correct value.

If we use either Eq. (34) or Eq. (35), we find the calculated bulk modulus (the reciprocal of the compressibility) of iron to be 1.7×10^{12} dyne/cm^2, in exact agreement with experiment.[49] The closeness of the agreement has no real significance, because the bulk modulus is quite sensitive to small changes in the calculated energy points. In particular, the uncertainty attached to the energy for $r_s=3.10$ will have a major effect on the bulk modulus. If we do not accept the least-squares fit in Table VI when $r_s=3.10$, but use the energy for $n_{4s}=1.0$, we approximately double the calculated bulk modulus. On the other hand the cohesive energy and the equilibrium value of r_s are less radically affected. In spite of this uncertainty, the calculated bulk modulus adds some support to our feeling that the work presented here is a valid first approximation to the cohesive energy of metallic iron. For convenience, we list some of our results in Table VII.

TABLE VII. Summary of the energy calculation results.

	Calculated	Observed
Cohesive energy (ry/atom)	0.43±0.2	0.32[a]
Atomic sphere radius, r_s (Bohr radii)	2.66±0.1	2.66[b]
Bulk modulus (dyne/cm^2)	1.7–3×10^{12}	1.73×10^{12} [c]
Number of 4s electrons per atom, n_{4s}	1.0±0.3	

[a] See reference 48.
[b] See reference 29.
[c] See reference 49.

Note that the calculated energy differences between configurations of the free iron atom are in error by as much as 0.3 ry.[20] This suggests that a definitive calculation of the cohesive energy of metallic iron must be preceded or accompanied by a successful calculation for the low configurations of the free atom.

6. EXCHANGE ENERGY FOR A DETERMINANT WAVE FUNCTION

In this section we make a crude estimate of the exchange energy as calculated from a determinant wave function. The treatment of Secs. 1–5 replaced the exchange and correlation holes about each electron by a Coulomb hole centered at the middle of the cell in which the electron moves. This approximation, although it is not a correct description of the actual situation, has the advantage of being correct at the limit of large lattice constants, and of being practicable at all lattice constants. We do not evaluate the expectation value of the total energy for a specific wave function for the solid. Thus we cannot say that the energy we find for the solid is an upper limit of the true energy.

In the treatment which follows, we find the exchange energy for the solid using a single determinant wave function and rather severe approximations. The principal restriction is that we ignore all Slater integrals[45] other than $F^0(a,b)$, the direct Coulomb interaction of

[48] Edwards, Johnston, and Ditmars, J. Am. Chem. Soc. **73**, 4729 (1951), give the heat of sublimation of iron at 0°K as 99.2±0.1 kcal/mole, which is equivalent to 0.32 ry/atom.

[49] *The American Institute of Physics Handbook* (McGraw-Hill Book Company, Inc., New York, 1957), pp. 2–56, gives the elastic stiffness constants of iron as $c_{11}=2.37$, $c_{12}=1.41$, $c_{44}=1.16$, all in units of 10^{12} dyne/cm^2. Thus the bulk modulus, which equals $\frac{1}{3}(c_{11}+2c_{12})$, is 1.73×10^{12} dyne/cm^2.

the spherically symmetric parts of the charge distributions of electrons a and b. We also assume a number of orthogonality conditions which are valid only at very large lattice constants.

The determinant wave function of the solid is:

$$\Psi = (N!)^{-\frac{1}{2}} \det|f_{a\mathbf{k}}(\mathbf{r})|, \tag{36}$$

where

$$f_{a\mathbf{k}}(\mathbf{r}) = M^{-\frac{1}{2}}\Psi_a(\mathbf{k},\mathbf{r}). \tag{37}$$

Here the $\Psi_a(\mathbf{k},\mathbf{r})$ are one-electron Bloch wave functions normalized to 1 in the unit cell, and M is the number of atoms in the crystal. The total number of wave functions which appears in (36) is $N=MZ$, where Z is the number of valence electrons per atom. Each space orbital, described by a band quantum number a and a wave vector $\mathbf{k}$, appears twice, once with each of two spin directions. Wave functions belonging to different wave vectors are orthogonal, and we further assume that the wave functions of different bands for the same wave vector $\mathbf{k}$ are also orthogonal. This is not strictly true for the wave functions used in our work, although linear combinations of these wave functions which are orthogonal can be chosen. We have, with our approximations:

$$\int_L f_{a\mathbf{k}}(\mathbf{r}) f_{a'\mathbf{k}'}(\mathbf{r}) d\tau = \delta_{aa'}\delta_{\mathbf{k}\mathbf{k}'}, \tag{38}$$

and

$$\int_L \Psi^*\Psi d\tau_1 \cdots d\tau_N = 1, \tag{39}$$

where the subscript L indicates that the integration is over the entire lattice.

The energy of the crystal (excluding the internal energy of the ion cores) is:

$$E(\text{crystal}) = \int_L \Psi^* H \Psi d\tau_1 \cdots d\tau_N. \tag{40}$$

Here the Hamiltonian H is:

$$H = \sum_{i=1}^{N} T(\mathbf{r}_i) + \sum_{i=1}^{N}\sum_{\mathbf{r}_n} v(\mathbf{r}_i - \mathbf{r}_n) + \tfrac{1}{2}{\sum_{i,j}}' 2|\mathbf{r}_i - \mathbf{r}_j|^{-1} + \tfrac{1}{2}{\sum_{n,m}}' 2Z^2|\mathbf{r}_n - \mathbf{r}_m|^{-1}. \tag{41}$$

In Eq. (41) the $\mathbf{r}_i$ and $\mathbf{r}_j$ give the positions of the N valence electrons, and the $\mathbf{r}_n$ and $\mathbf{r}_m$ give the positions of the M ion cores, which have charge Z and are assumed to be nonoverlapping. The first term in (41) is the total kinetic energy operator for the valence electrons. The second term gives the interaction of the valence electrons with the ion cores, while the third and fourth terms give the interaction of the electrons, and of the ion cores, among themselves. The primed sums exclude terms with vanishing denominators.

The total energy of the crystal, based on approximations equivalent to those made in earlier parts of the paper, can be written:

$$E(\text{crystal}) = 2\sum_{a\mathbf{k}} \int_C \Psi_{a\mathbf{k}}^*(\mathbf{r})[T(\mathbf{r}) + v(\mathbf{r})]\Psi_{a\mathbf{k}}(\mathbf{r}) d\tau + 2M \sum_a \sum_{a'} p_a p_{a'} F_{aa'} + E(\text{exchange}). \tag{42}$$

Here the integration is over the cell at the origin. $F_{aa'}$ is the average interaction energy of an electron in band a with an electron in band a', where both electrons have unit charge in the atomic cell in the solid, as in Eq. (31). We have introduced the quantity p_a in (42) to represent the fractional occupation of band a; for a full band, $p_a=1$. There are six bands occupied in our calculation: five $3d$ bands and the $4s$ band.

The third term in (42) gives the exchange effects which replace the Coulomb hole that was used in our main calculation. It is the exchange term which is most difficult to evaluate. The formal expression is easily written. We have:

$$E(\text{exchange}) = -M^{-2}\sum_{a,a',\mathbf{k},\mathbf{k}'} \times \int 2\Psi_{a\mathbf{k}}^*(\mathbf{r})\Psi_{a'\mathbf{k}'}(\mathbf{r})\Psi_{a\mathbf{k}}(\mathbf{r}')\Psi_{a'\mathbf{k}'}^*(\mathbf{r}') \times |\mathbf{r}-\mathbf{r}'|^{-1} d\tau d\tau'. \tag{43}$$

The sums over a and $\mathbf{k}$, and over a' and $\mathbf{k}'$, each extend over all occupied states in the crystal.

To reduce (43) to a tractable form, we separate it into a part representing the integral within an atomic polyhedron and part giving the interaction between polyhedra. If we also assume that the charge density in each cell is sharply peaked near the nucleus (this means that the exchange energy of $4s$ electrons must be estimated separately), that the orthogonality condition (38) holds, and that all terms corresponding to higher Slater integrals are to be ignored, then we get contributions to the exchange energy only for $a=a'$.[50] In this case the interaction within lattice cells gives:

$$-M^{-1}\sum_{a,\mathbf{k},\mathbf{k}'} F_{aa} = -M\sum_a p_a^2 F_{aa}. \tag{44}$$

The interaction between different lattice cells gives, approximately:

$$-M^{-1}\sum_{a,\mathbf{k},\mathbf{k}'}{\sum_{\mathbf{r}_m,\mathbf{r}_n}}' 2|\mathbf{r}_n-\mathbf{r}_m|^{-1}\exp[i(\mathbf{k}-\mathbf{k}')\cdot(\mathbf{r}_n-\mathbf{r}_m)] = -M^{-1}\sum_a{\sum_{\mathbf{R}}}'2[\sum_{\mathbf{k}}\exp(i\mathbf{k}\cdot\mathbf{R})]^2/R. \tag{45}$$

The transition from the first line of (45) to the second line follows if we substitute the lattice vector $\mathbf{R}$ for

[50] Our treatment of the exchange energy to this point is closely similar to the treatment given by J. C. Slater, Phys. Rev. **49**, 537 (1936). We arrive at rather different results, however.

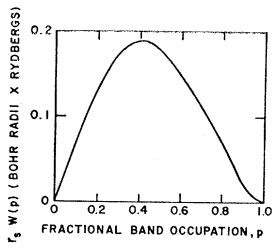

FIG. 5. The exchange contribution $W(p)$, multiplied by r_s, is shown as a function of fractional band occupation. See Eq. (46).

$\mathbf{r}_n-\mathbf{r}_m$, and note that a state with wave vector $-\mathbf{k}$ is occupied when the state with wave vector $\mathbf{k}$ is occupied. The sum over $\mathbf{k}$ in the second line of (45) is extended over all occupied states in band a, and a is summed over the five $3d$ bands. If we introduce the notation:

$$W(p_a)=M^{-2}\sum_{\mathbf{R}}{}'\,2[\sum_{\mathbf{k}}\exp(i\mathbf{k}\cdot\mathbf{R})]^2/R, \qquad (46)$$

then the exchange energy of the crystal can be written:

$$E(\text{exchange},3d)=-M\sum_a[p_a^2F_{aa}+W(p_a)]. \qquad (47)$$

We have implied that W is a function of a single parameter p_a, the fractional filling of band a. This is only an approximation, since the value of the sum in (46) depends on the way the band is filled. Some general statements about the form of W can be made by inspection of (46). In particular, W will vanish for a full band, because $\sum\exp(i\mathbf{k}\cdot\mathbf{R})$ over a full band equals zero; note that $\mathbf{R}=0$ is excluded.

We have evaluated $W(p)$ for a band in a simple cubic crystal, assuming that the filled states occupy a cubic region centered at the origin of the Brillouin zone. Under these circumstances the sum in (46) is quite simple. The result is shown in Fig. 5.

This completes the formal evaluation of the exchange energy, which we have carried out under rather severe approximations. It is of some interest to see how the energy of the exchange hole, Eq. (47), compares with the energy of the Coulomb hole used in Sec. 5. There each electron in a lattice cell is assumed to interact with the remaining seven electrons in the cell, rather than with the total valence charge density. The energy of the resulting Coulomb hole is the difference in energy between the 32 valence-electron interactions given in the second term of (42), and the 28 interactions included in Eq. (30). In particular, for the $3d^74s$ configuration of the solid we have, for the energy of the Coulomb hole,

$$[(49/2)F_{dd}+7F_{sd}+\tfrac{1}{2}F_{ss}]-[21F_{dd}+7F_{sd}] \equiv(7/2)F_{dd}+\tfrac{1}{2}F_{ss}. \qquad (48)$$

We use values for $r_s=2.66$, and take $F_{dd}=1.381$ from Table V. For F_{ss} we use the approximate value $2.4/r_s=0.902$ which applies to a uniform charge distribution. The Coulomb hole thus contributes 5.285 ry to the cohesive energy found in Sec. 5.

To find the energy of the exchange hole, we need the values of the fractional occupations of the five $3d$ bands. For the configuration $3d^74s$ these can be found from the one-electron energies of Sec. 4. Two of the $3d$ bands are completely filled, and the fractional occupations of the three remaining bands are 0.84, 0.34, and 0.32. For these values we have $\sum p_a^2=2.924$, and $\sum W(p_a)=0.405/r_s$. The total $3d$ contribution to the exchange hole is 4.190 ry.

The approximations which led to (47) fail completely for $4s$ electrons. We use the free-electron approximation to find the $4s$ exchange energy, which gives $0.916/r_s=0.344$ ry. The total exchange hole for the valence electrons is 4.534 ry, which is about 0.75 ry less than the Coulomb hole. Thus the energy of the solid as evaluated from a single determinant wave function is higher by 0.75 ry, for $r_s=2.66$ and $n_{4s}=1.0$, than the energy found from the approximations used in Sec. 5. This means that the determinant wave function will probably not give a positive cohesive energy for the solid. A complete analysis would require evaluation of Eq. (42) for various values of r_s and n_{4s} to find the minimum energy of the solid relative to that of the free atom.

A source of error in our evaluation of the exchange energy, Eq. (47), should be pointed out. The value of F_{dd} we use is averaged over all occupied states in the $3d$ band. Had we taken into account the fact that F_{dd} is smaller for the states near the bottom of the $3d$ band, for which p_a is large, we would have found a smaller exchange hole.

We have estimated the contribution of correlations to the cohesive energy by using an effective correlation potential.[51] The correlation energy calculated in this way has almost as big a value in the iron atom as in the atomic cell of the solid. Thus the net effect on the cohesive energy is quite small. We estimate that these correlation effects contribute less than 0.1 ry per atom to the cohesive energy of iron.

Our result for the exchange hole does not contribute a large enough amount to the cohesive energy. This is an old problem for solids with partially filled bands.[16] A single determinant wave function does not adequately describe solids in which wave functions on neighboring atoms overlap very little; it gives too great an ionic component in the wave function.

We have assumed throughout this work that each orbital state is filled with two electrons or with none. If we relax this restriction, an increase in the population of electrons with one spin direction and a corresponding decrease in the population of electrons with the other spin direction will generally lead to an increase in the magnitude of the exchange energy. This decrease in the energy of the crystal must be weighed against the other changes in energy which accompany changes in the occupation of the bands. It would be relatively easy to explore this somewhat further, but the validity of such a calculation is open to question in view of the rather poor energy value which the single determinant method gives for the solid in the singlet state.

[51] P. Gombás, Acta Phys. Hung. 4, 187 (1954); H. Mitler, Phys. Rev. 99, 1835 (1955).

7. CONCLUSION

Our result for the cohesive energy of body-centered cubic iron, given in Sec. 5, is in satisfactory agreement with experiment. It demonstrates the practicability of cohesive energy calculations for many-electron systems like the transition metals, which have been practically unexplored heretofore. The modified tight-binding method developed in Secs. 2 and 4 promises to be a useful tool for studying narrow energy bands in solids. But a rigorous treatment of exchange and correlation effects for solids whose valence electrons deviate substantially from free-electron behavior is still needed.

Extensions and improvements which might be made to our present work are easily found. A more sophisticated treatment of the overlap contribution to the wave function, perhaps along lines indicated by Löwdin,[7] might be considered. Considerable accuracy would be gained by increasing the number of terms retained in the expansion of the overlap contribution. If a calculation using more accurate wave functions were made, it would become desirable to remove the off-diagonal elements of the Hamiltonian, and to include the possibility of admixture of $4p$ states into the valence bands. A considerably more ambitious undertaking would be a calculation for the solid based on atomic Hartree-Fock functions and including all Slater integrals. The higher Slater integrals within a single lattice cell can be calculated by tedious, but straightforward, extensions of the methods developed in this work. On the other hand the correct treatment of exchange integrals involving different lattice cells is more difficult. If higher Slater integrals are to be included, the nonspherical shape of the atomic polyhedron must also be taken into account.

The simple form of the modified tight-binding wave functions found for iron suggests that they might profitably be used in a study of the x-ray scattering amplitude in the solid.[28]

8. ACKNOWLEDGMENTS

The author is grateful to Professor Eugene P. Wigner for many valuable suggestions and for his continuing interest and encouragement. He is indebted to the National Science Foundation and to Princeton University for financial support during early stages of this work, and thanks Dr. Earl Callen, Professor Richard A. Ferrell, and Dr. Conyers Herring for helpful comments.

APPENDIX A. TESTING THE ACCURACY OF TRUNCATED PLANE WAVE EXPANSIONS

In order to estimate the accuracy to be expected from our modified tight-binding approximation for $4s$ electrons in iron, we calculate the energy for various approximate expansions of free electron wave functions. Thus we carry out a simple variant of the empty lattice test, which was first used by Shockley.[52]

The Bloch wave function for a free electron with wave vector $\mathbf{k}$ is $\exp(i\mathbf{k}\cdot\mathbf{r})$, and its energy is k^2 in our units. The plane wave can be expanded in spherical harmonics, giving:

$$\exp(i\mathbf{k}\cdot\mathbf{r})=\sum_l i^l(2l+1)j_l(kr)P_l(\eta), \qquad \text{(A1)}$$

where η is the cosine of the angle between $\mathbf{k}$ and $\mathbf{r}$, $P_l(\eta)$ is a Legendre polynomial of order l, and $j_l(kr)$ is a spherical Bessel function of order l.[53]

The approximation we want to test replaces the accurate free electron wave function, Eq. (A1), by another in which the summation includes only terms with $l\leq n$, and in which the wave function is defined only within a sphere of radius r_s, rather than in all space. Since the wave function is now confined to a finite region, we use the boundary correction of Eq. (27) in calculating the energy of the approximate wave function, and find

$$E=k^2\left(1-\frac{(2/kr_s)(n+1)j_n(kr_s)j_{n+1}(kr_s)}{\sum_{l=1}^{n}(2l+1)\{[j_l(kr_s)]^2-j_{l-1}(kr_s)j_{l+1}(kr_s)\}}\right). \qquad \text{(A2)}$$

Since we confine the wave function in a sphere, rather than in the atomic polyhedron, we cannot expect to find the proper behavior at the surface of the Brillouin zone. In Fig. 5 we show the energies calculated from Eq. (A2) for values of k out to the edge of an imaginary spherical Brillouin zone holding two electrons per atom. The occupation of the band is related to k by the expression

$$N(k)=4(kr_s)^3/9\pi, \qquad \text{(A3)}$$

where $N(k)$ is the number of electrons per atom with wave vector $\leq k$. Thus $k=2.418r_s^{-1}$ corresponds to a filled band, and $k=1.919r_s^{-1}$ corresponds to a half-filled band, i.e. one electron per atom.

For our purpose, a reasonable measure of the accuracy of the truncated plane wave expansions is their accuracy for a half-filled band, since this is close to the actual situation in iron. We see from Fig. 6 that keeping terms through second order gives an error of 5% in the energy at the point where the band is half-filled, while keeping third-order terms reduces this error to less than 0.5%.

We have also tested a still cruder approximation to the accurate plane wave expansion. This replaces the spherical Bessel functions by the first few terms of their power series expansion[53]

$$j_l(x)=2^l x^l\sum_q(l+q)!(-x^2)^q/q!(2l+2q+1)!. \qquad \text{(A4)}$$

[52] W. Shockley, Phys. Rev. **52**, 866 (1937).

[53] J. A. Stratton, *Electromagnetic Theory* (McGraw-Hill Book Company, Inc., New York, 1941), pp. 404–406.

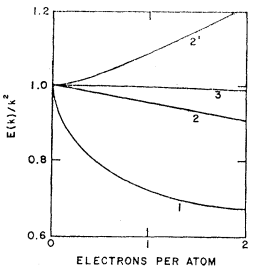

FIG. 6. The energy of truncated expansions of plane waves with wave vector k is shown in units of the exact free electron energy. The abscissa gives the number of electrons per atom contained in a spherical Brillouin zone of radius k. The curves marked 1, 2, and 3 refer, respectively, to truncated expansions whose highest spherical harmonic has angular momentum $l=1$, 2, or 3. The curve marked 2′ refers to an expansion containing spherical harmonics through $l=2$, in which the radial functions have been truncated; see Eq. (A5).

We find reasonably good energy values with a rather small number of terms. For small values of k it is necessary to keep more terms in the expansion of $j_l(kr)$ for low values of l than for higher values of this parameter. In particular, if the fractional error in energy for small k is to be of the order of $(kr_s)^{2n}$, we must keep all Legendre polynomials of order $l\leq n$, and the coefficient of $P_l(\eta)$ need contain powers of kr only through $(kr)^{2n-l}$. Thus only one term is necessary for the coefficient of the highest Legendre polynomial retained, while $n+1$ terms should be kept in the expansion of $j_0(kr)$. The simplest wave function whose fractional energy error for small values of k is of the order of $(kr_s)^4$ is

$$f(\mathbf{k},\mathbf{r})=\left(1-\frac{k^2r^2}{6}+\frac{k^4r^4}{120}\right)+i\left(kr-\frac{k^3r^3}{10}\right)\eta-\frac{k^2r^2}{3}\frac{3\eta^2-1}{2}. \quad \text{(A5)}$$

The energy of this wave function is shown as the top curve in Fig. 6. It is in error by about the same amount, though in the opposite direction, as the wave function containing the complete expressions for j_0, j_1, and j_2.

The energies of our trial wave functions have been evaluated in a spherical lattice cell and consequently give a spherically symmetric band in an assumed spherical Brillouin zone. Nevertheless, Fig. 6 gives considerable information about the number of terms needed when free-electron wave functions are expanded in a single cell of the lattice. We make use of these results in Sec. 2.3, where we use the same number of terms for the modified tight-binding wave function of 4s electrons in iron as is kept in (A5).

APPENDIX B. CONTRIBUTION OF DISTANT NEIGHBORS TO THE 4s WAVE FUNCTION

Because of the large overlap of the wave functions of 4s electrons in iron, it is necessary to sum contributions from distant neighbors in finding the tight-binding wave function for the 4s band. We have carried out the explicit sums through sixth-nearest neighbors, but require an approximate method for finding the contribution of more distant neighbors. The method we use is rather crude; at the end of this appendix a more refined method is mentioned.

We wish to evaluate the sum

$$\Phi_0''(\mathbf{k},\mathbf{r})=\sum{}'' \exp(i\mathbf{k}\cdot\mathbf{r}_n)R_{4s}(\mathbf{r}-\mathbf{r}_n), \quad \text{(B1)}$$

which is restricted to lattice points $\mathbf{r}_n$ beyond some fixed distance. Our basic approximation is to replace the summation by an integration, thus assuming the lattice points to be smeared out in space. If t_0 is the radius of a sphere enclosing all the atoms for which the summation has been carried out exactly,[54] then the approximate contribution of the remaining atoms to the tight-binding wave function is

$$\Phi_0''(\mathbf{k},\mathbf{r})=(3/4\pi r_s^3)\times\int_{t_0}^{\infty}\exp(ikt\eta')R_{4s}(\mathbf{r}-\mathbf{t})t^2dtd\eta'd\phi, \quad \text{(B2)}$$

where η' is the cosine of the angle between $\mathbf{k}$ and $\mathbf{t}$.

The accuracy with which we evaluate Eq. (B2) depends in part on the approximations we wish to make for $R_{4s}(\mathbf{r}-\mathbf{t})$. We used

$$R_{4s}(\mathbf{r}-\mathbf{t})\sim B\exp(-b|\mathbf{r}-\mathbf{t}|)\sim B\exp(-bt+br\eta''), \quad \text{(B3)}$$

where η'' is the cosine of the angle between $\mathbf{r}$ and $\mathbf{t}$. The second step in (B3) represents a further approximation, but not a serious one, since $r\leq r_s$, $t\geq t_0$, and $t_0\gg r_s$.

The exponentials in Eqs. (B2) and (B3) can now be expanded in spherical harmonics, giving[55]

$$\exp(ikt\eta')=\sum_{l=0}^{\infty}(2l+1)i^l j_l(kt)P_l(\eta'), \quad \text{(B4)}$$

$$\exp(br\eta'')=\sum_{m=0}^{\infty}(2m+1)i_m(br)P_m(\eta''). \quad \text{(B5)}$$

Here $j_l(kt)$ is the spherical Bessel function already encountered in Appendix A,[53] and $i_m(br)$—which should not be confused with $i=\sqrt{-1}$—is another spherical Bessel function defined by[56]

$$i_m(z)=i^{-m}j_m(iz)=(\pi/2z)^{\frac{1}{2}}I_{m+\frac{1}{2}}(z)=(2z)^m\sum_{p=0}^{\infty}[z^{2p}(p+m)!/p!(2m+2p+1)!]. \quad \text{(B6)}$$

[54] If the exact summation has included the nearest G neighbors plus the atom at the origin, then $t_0=(G+1)^{\frac{1}{3}}r_s$.

[55] G. N. Watson, *A Treatise on the Theory of Bessel Functions* (Cambridge University Press, London, 1945), second edition, Sec. 11.

[56] The Bessel function of imaginary argument, $I_n(z)$, is discussed in Sec. 3.7 of reference 55.

With the foregoing approximations and expansions, and with use of the addition theorem for Legendre polynomials, Eq. (B2) reduces to

$$\Phi_0''(\mathbf{k},\mathbf{r})=3Br_s^{-3}\sum_{l=0}^{\infty} i^l(2l+1)i_l(br)P_l(\eta) \times\int_{t_0}^{\infty} t^2 j_l(kt)\exp(-bt)dt, \quad \text{(B7)}$$

where η is the cosine of the angle between $\mathbf{k}$ and $\mathbf{r}$.

We have used Eq. (B7) to find the approximate contribution of atoms beyond sixth-nearest neighbors to the tight-binding wave function in iron. The parameters we used are: $t_0=(65)^{\frac{1}{3}}r_s$, $B=1.471$(Bohr radii)$^{-\frac{1}{2}}$, $b=0.575$(Bohr radii)$^{-1}$; R_{4s} was normalized to 4π. No attempt was made to calculate the integral in Eq. (B7) with great accuracy. In keeping with the approximations made in Sec. 2.3 and discussed in Appendix A, we keep only the following terms of $i_l(br)$:

$$\begin{gathered} i_0(br)=1+(b^2r^2/6)+(b^4r^4/120), \\ 3i_1(br)=br+(b^3r^3/10), \quad 5i_2(br)=b^2r^2/3. \end{gathered} \quad \text{(B8)}$$

The angular part of the wave function for the three symmetry directions is

direction	$P_1(\eta)$	$P_2(\eta)$
⟨001⟩	$Y_{13}/\sqrt{3}$	$Y_{22}/\sqrt{5}$
⟨111⟩	$Y_{14}/\sqrt{3}$	$Y_{26}/\sqrt{5}$
⟨110⟩	$Y_{11}/\sqrt{3}$	$(\sqrt{3}Y_{21}-Y_{22})/2\sqrt{5}$.

(B9)

These spherical harmonics are defined in Table II. The tight-binding wave functions formed from spherically symmetric atomic orbitals must belong to the representations with subscript 1 in Table I. A comparison of (B9) with Tables I and II shows that this is the case. It is interesting that for the ⟨110⟩ direction we find a linear combination of the two second order spherical harmonics, Y_{21} and Y_{22}, which belong to the representation Σ_1. These two harmonics also appear in the exact summations over the near neighbors, and their coefficients are approximately in the ratio $\sqrt{3}:-1$ given by (B9).

Because we smear the distant lattice points uniformly, the requirement of Table I that the coefficients of the first- and second-order spherical harmonics in $\Phi_0(\mathbf{k},\mathbf{r})$ vanish when $\mathbf{k}$ is at the endpoints of the three symmetry directions[57] cannot be exactly fulfilled in Eq. (B2). These coefficients do, however, go through zero for a value of k near the surface of the Brillouin zone. We have set the distant-neighbor portion of the $4s$ wave function in the solid equal to zero where that is required by symmetry.

The preceding discussion gives the procedures used in our work to find the contribution of distant neighbors to the tight-binding $4s$ wave function in iron. The remainder of the description of that wave function is given in Sec. 2.3. We conclude by referring to a somewhat more accurate treatment which might be used to eliminate the approximation made in Eq. (B3). If, for large distances, we used

$$R_{4s}(\mathbf{r}-\mathbf{t})=B|\mathbf{r}-\mathbf{t}|^{m-1}\exp(-b|\mathbf{r}-\mathbf{t}|), \quad \text{(B10)}$$

we could make use of the expansion[58]:

$$|\mathbf{r}-\mathbf{t}|^{m-1}\exp(-b|\mathbf{r}-\mathbf{t}|) =b^{-m}(rt)^{-\frac{1}{2}}\sum_{l=0}^{\infty}(2l+1)\zeta_{m,l}(br,bl)P_l(\eta''). \quad \text{(B11)}$$

Some of the properties of the $\zeta_{m,l}$ have been given by Barnett and Coulson,[58] and might form the basis of a more rigorous treatment than the one given here.

[57] The coefficients of the second-order spherical harmonics in $\Phi_0(\mathbf{k},\mathbf{r})$ need not vanish when $\mathbf{k}$ is at the endpoint of ⟨110⟩.

[58] M. P. Barnett and C. A. Coulson, Phil. Trans. Roy. Soc. London **A243**, 221 (1951). See also Sec. 6.1.2 of reference 7.